VASCULAR COUPLING DEVICE FOR END-TO-END ANASTOMOSIS

by

Huizhong Li

A dissertation submitted to the faculty of
The University of Utah
in partial fulfillment of the requirements for the degree of

Doctor of Philosophy

Department of Mechanical Engineering

The University of Utah

August 2015

The University of Utah Graduate School

STATEMENT OF DISSERTATION APPROVAL

The dissertation of **Huizhong Li**

has been approved by the following supervisory committee members:

Bruce K. Gale	, Chair	**5/14/2015** Date Approved
Jayant Agarwal	, Member	**5/14/2015** Date Approved
Kenneth L. Monson	, Member	**5/14/2015** Date Approved
James R. Stoll II	, Member	**5/14/2015** Date Approved
Bart Raeymaekers	, Member	**5/14/2015** Date Approved

and by **Tim Ameel**, Chair/Dean of

the Department/College/School of **Mechanical Engineering**

and by David B. Kieda, Dean of The Graduate School.

ABSTRACT

In microsurgical operating room environments, it is often necessary to cut and reattach vessels multiple times during surgery. The current method of vascular anastomosis is hand suturing. This technique is time consuming, difficult, and requires complex instruments. To solve this problem, researchers have explored alternative ways to improve this technique. Typical examples are staples, clips, cuffing rings, adhesives, and laser welding. The potential of these techniques has been hindered due to the lack of biocompatibility, complex procedures for use, and general inefficiency. As a result, few of these devices have been commercialized.

One promising alternative is a ring-pin coupling device. This device has been shown to be useful for venous anastomosis, but lacks the versatility necessary for arterial applications. One purpose of this study was to optimize a vascular coupling design that could be used for arteries and veins of various sizes. To achieve this, finite element analysis was used to simulate the vessel-device interaction during anastomosis. Parametric simulations were performed to optimize the number of pins, the wing pivot point, and the pin offset of the design. The interaction of the coupler with various blood vessel sizes was also evaluated.

The optimal vascular coupling device has four rotatable wings and one translatable spike in each wing. Prototypes were manufactured using polytetrafluoroethylene (PTFE) and high-density polyethylene (HDPE). A set of installation tools was designed

to facilitate the anastomosis process. Proof-of-concept testing with the vascular coupler using plastic tubes and porcine cadaver vessels showed that the coupler could be efficiently attached to blood vessels, did not leak after the anastomosis was performed, had sufficient joint strength, and had little impact on flow in the vessel. A simplified finite element model assisted in the evaluation of the tearing likelihood of human vessels during installation of the coupler. The entire anastomosis process can be completed in three minutes when using the vascular coupler to join porcine cadaver vessels.

A metal-free vascular coupling system that can be used for both arteries and veins was designed, fabricated, and tested. A set of corresponding instruments were developed to facilitate the anastomosis process. Evaluation of the anastomosis by Scanning Electron Microscopy (SEM) and Magnetic Resonance Imaging (MRI) demonstrated that the installation process does not cause damage to the vessel intima and the vascular coupling system is not exposed to the vessel lumen. Mechanical testing results showed that vessels reconnected with the vascular coupling system could withstand 12.7±2.2 N tensile force and have superior leak profiles compared to hand sutured vessels. The anastomotic process was successfully demonstrated on both arteries and veins in cadaver and live pigs.

TABLE OF CONTENTS

ABSTRACT iii

ACKNOWLEDGEMENTS vii

CHAPTERS

1 INTRODUCTION 1

Microsurgery 1
State of the Art: Hand Suturing 2
History of Sutureless Anastomoses 3
Mechanical Devices for Vascular Anastomoses 4
Non-device-based Technologies for Vascular Anastomoses 14
Sutureless Anastomoses in Clinical Application 16
Motivation and Prior Design 17
Chapter Outlines 19
References 20

2 OPTIMIZATION AND EVALUATION OF A VASCULAR COUPLING DEVICE FOR END-TO-END ANASTOMOSIS: A FINITE ELEMENT ANALYSIS 26

Abstract 26
Introduction 27
Materials and Methods 30
Results 37
Discussion 42
Conclusion 44
References 44

3 A NEW VASCULAR COUPLER DESIGN FOR END-TO-END ANASTOMOSIS: FABRICATION AND PROOF-OF-CONCEPT EVALUATION 47

Abstract 48
Introduction 48

Materials and Methods 49
Results 53
Discussion 56
Conclusion 56
Acknowledgements 57
References 57

4 A NOVEL VASCULAR COUPLING SYSTEM FOR END-TO-END ANASTOMOSIS 59

Preliminary Design and Testing 59
Final Design and Development 64

5 INITIAL LIVE ANIMAL STUDY 74

Abstract 74
Materials and Methods 74
Results 76
Discussion and Conclusion 76

6 CONCLUSIONS, CONTRIBUTIONS, AND FUTURE WORK 79

Conclusions 79
Contributions 81
Future Work 82

ACKNOWLEDGEMENTS

There are a number of people I would like to thank for their great help on this work. I would like to express my appreciation to those who raised, taught, mentored, and loved me over the years.

First, I would like to thank my advisor Dr. Bruce Gale for his valuable guidance and support. I am very grateful I met him when starting my 20s and have learned many precious research and life lessons from him. I appreciate and cherish the trust and motivation from him and will carry them with me wherever I go in my future life. I also would like to thank Dr. Jay Agarwal for his funding support and inspirations. I am grateful for his time and effort to provide a "cool" project and many good ideas. I would like to thank my supervisory committee Dr. Ken Monson, Dr. Rob Stoll, and Dr. Bart Raeymaekers for their insights and suggestions.

I would like to thank Dr. Himanshu Sant, Dr. Jill Shea, and Dr. Brittany Coats for their help on this work. I would like to thank Ilya Zhuplatov, Patti Larrabee, and Hannah Beal for their help to harvest tissues for me and Dr. Christi Terry and Dr. Yuxia He for their time and help on the animal study. I would like to thank all members of the State of Utah Center of Excellence for Biomedical Microfluidics for their constant support and the enjoyable lab environment.

More importantly, I would like to thank my parents for their endless love and unconditional support. I would like to thank my husband Xiaojun Sun for his constant

love and support. I am grateful to him for providing me an amazing life. Lastly, I would like to express my appreciation for all the blessings I have received.

CHAPTER 1

INTRODUCTION

Microsurgery

During the past decades, the development of microsurgery has brought great change to the field of reconstructive surgery in both research and clinical areas [1]. According to statistics from the American Society of Plastic Surgeons, almost 12 million reconstructive surgeries were performed in 2013 to help patients with abnormal structures on the body [2]. Many of these were microsurgeries where the use of an operating microscope in microsurgery provides surgeons the magnification that allows more accurate and consistent surgical procedures [3]. Common microsurgical procedures are replantation and free tissue transfer. Replantation is the reattachment of body parts such as fingers and thumbs [4]. Free tissue transfer is a reconstructive procedure that takes a section of tissue from a healthy part of the body and transfers it to an area that needs to be repaired [5]. During both procedures, arteries and veins from the donor tissue are cut and then reattached at the reconstruction site [6]. These surgical vascular repair processes are called vascular anastomoses. In order to ensure the success of replantation and free tissue transfer surgeries, good quality vascular anastomoses are necessary.

State of the Art: Hand Suturing

Vascular anastomoses are not only used by plastic surgeons for reconstructive surgeries, but also for other procedures, including cardiac surgery, vascular surgery, and neurosurgery [7]. Regardless of the vessel sizes in different procedures and the specific technique employed, the standard technique for performing vascular anastomosis is hand suturing, which was developed by Alexis Carrel in 1902. He developed the method of using round-bodied needles to minimize invasive intima and performed an anastomosis successfully [8]. When Jules Jacobson carried out the first vascular surgery during which two 1.4 mm vessels were connected with microscope assistance, the penetrating suture with attached needles became the gold standard for microvascular anastomosis [9]. In 1966, Buncke performed a successful surgery which realized an ear replantation in rabbits by connecting 1 mm diameter vessels [10]. Then in 1968, the first human microsurgical replantation of toe to thumb was reported by Cobbett [11]. Thousands of related surgeries have now been performed.

There are six primary suture techniques used in reconstructive and other surgeries: continuous suture, interrupted suture, locking continuous, continuous horizontal mattress, interrupted horizontal mattress with eversion, and sleeve anastomosis [12]. Among these methods, interrupted suture is the most common technique. Usually this technique uses a monofilament nylon suture mounted on sharp round-bodied needles [13]. Even now, because hand suturing provides reliable anastomosis and good long-term results, it is still frequently used in microvascular surgeries both for end-to-end and end-to-side anastomosis [14].

There are a variety of reasons why suturing may no longer be the best option for

performing anastomoses. The surgical environment has become more and more challenging over the past few years with the introduction of minimally invasive approaches, which has led to some limitations on standard vascular anastomoses, since it is difficult to perform hand suturing through small incisions [14]. In addition, traditional hand suturing is quite time consuming and tedious. It requires very skillful surgeons and uses complex lab instruments [15]. It is also common that the loose end of the suture falls into the operative field during surgery, which leads to extended surgeries or even surgery suspension since it can be hard to pick the suture up from the sticky operative field [16]. Even if everything goes well, for a surgery that needs to replant four crushed fingers, it can take 24 hours [17]. Hand suturing also induces errors, which include uneven spacing, inversion of suture walls, and intima misalignment, which can lead to leaks, thrombosis, and even death [18, 19]. The reported 2-6% anastomosis failure due to suturing errors may cause the failure of the whole reconstructive surgery and increase healthcare costs [18, 20, 21]. All of these factors suggest there may be better ways to perform a precise anastomosis than standard hand suturing techniques. Therefore, sutureless anastomoses are proposed to reduce operating time, reduce error, and improve success in these already complex operations.

History of Sutureless Anastomoses

The history of vascular anastomosis with sutureless approaches can date back to the 1890s. Many experimental studies related to connecting blood vessels came up at that time [22]. In 1894, Abbe performed an end-to-end anastomosis on the femoral arteries of dogs with an hour-glass-shaped intraluminal glass tubing [23]. The two ends of the

glass tubing were inserted into each vessel end respectively and a fine silk thread was used to tie the vessel end over the glass tube. In 1897, Nitze employed ivory rings, which were placed outside of the vessel, to perform anastomosis [24]. In 1898, rings made from rubber or decalcified bone were proposed by Gluck to perform anastomosis [25]. In 1900, Payr brought up a method for vessel repair using magnesium tubes [26]. Four years later, Payr described another coupling device including two flanged rings. Similar attempts also include silver tubes by Tuffier [27], cameral stents by Carrel [8], and rubber tubes by Ward [28]. In 1945, Blackmore and Lord reported an end-to-side technique using a vitallium tube [29]. These methods achieved limited success due to the problem of infection and thrombosis. In addition, the success of suture techniques limited the development of nonsuture techniques at that time.

However, since the 1950s, a variety of innovative technology assisted and sutureless vascular anastomoses has been brought up and provided new solutions to reconstructive surgery. These prior attempts at reducing the amount of time and improving the success rates of microvascular anastomoses over hand suturing can be divided into two main categories: mechanical devices and non-device-based technologies.

Mechanical Devices for Vascular Anastomoses

Both permanent implants and bioabsorbable devices have been explored for vascular anastomosis. Common permanent implants include staple devices, ring-pin devices, cuffing devices, clipping devices, and other recent developed devices. On the other hand, bioabsorbable devices have become more and more popular for their potential to fully degrade *in vivo*. Generally, permanent implants have superior

anastomotic tensile strength compared to bioabsorbable devices, but long-term implantation might cause chronic trauma and thrombosis [18]. The advantages and shortcomings of each device are described and discussed below.

Staple device

The concept of stapling for tissue bonding was brought up in 1908 [7]. Earlier staple devices had been used in gastrectomy and cardiac surgeries. Because of the cumbersome and heavy assemblies, the staple devices were not widely accepted until the middle of the 19th century when the application was mainly focused on vascular anastomosis. A staple device works by everting the vessel ends over cuffs and then connecting two ends together with metal staples [30]. The metallic staple used by Androsov in 1956 brought people's attention back to nonsuture techniques [31]. The working mechanism of this device is to insert multiple staples at the same time then bend the initial U shape into a B shape to secure the end-to-end anastomosis, as seen in Figure 1.1. After two years, Inokuchi developed an apparatus using tantalum staples for end-to-side anastomosis with the same concept, but leaks were reported [29]. In 1964, Zingg employed staples made of tantalum wire for artery anastomosis in dogs [32]. The problem with the staple device is the process of the 180° eversion of the vessel ends, which adds difficulties to the anastomosis [30]. Besides, the consumption of vessels is relatively large for a total eversion of vessel walls during an anastomosis.

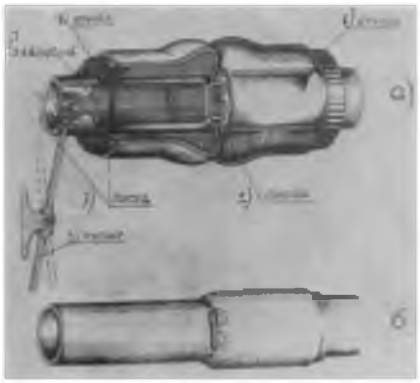

Figure 1.1. Mechanism of the staple device developed by Androsov [33]. (Reproduced with permission from *Microsurgery*, 1992)

Ring-pin device

The concept of a ring-pin device dates back to an even earlier time than staple devices. The devices were not suitable for smaller vessels until 1962, when Nakayama developed the modified ring-pin device that can be used for small diameter veins [34]. The device includes two metal rings. There are 6 pins and 6 pinholes evenly spaced for each ring. Unlike staple devices which require 180° eversion of the blood vessels, ring-pin devices make 90° eversion possible for vessels instead. When using the device, the physician places the ring around one end of vessel and then pins penetrate the vessel wall by everting the edge of the vessel onto the surface of the ring. The same procedure is applied on the other vessel. Once done, the physician connects the two rings together by inserting the pins of each ring into corresponding pinholes of the other [34]. It can be also applied for end-to-side anastomosis: For the "end" vessel, the procedure is the same with end-to-end; for the "side" vessel, a fine suture is needed to hook the device into the vessel and make sure the edge of the vessel is fixed on the pins of the ring [34].

An anastomosis instrument which preserves the advantages of Nakayama's device was developed by Ostrup in 1986. It is even better than Nakayama's device since it can work well on smaller vessels [30]. The instrument includes gauges which can measure the size of vessel diameter, a ring-pin holder, which is the main tool for performing anastomosis, a ring-pin, and microhooks used for mounting vessels on the pins on the ring [30]. This instrument is designed for both end-to-end and end-to-side anastomosis. Figure 1.2 shows the ring-pin device developed by Ostrup. The problem with ring-pin devices is that they are normally used for veins but less on arteries, because the artery usually slips off the pins during the installation process due to the arterial wall's elasticity and thickness. Rubber bands can be used to secure the artery to the individual pins, but it adds to the complexity of the whole process.

Cuffing device

An absorbable anastomosis cuff-coupler was brought up by Daniel in 1984 [27]. The cuff-coupler is made with two cuffs and a connecting collar. Modern injection

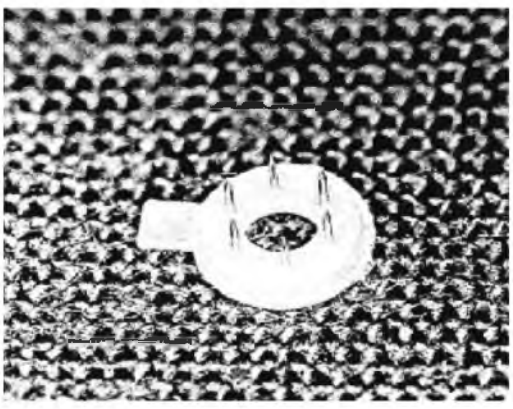

Figure 1.2. Ring-pin device developed by Ostrup [30]. (Reprinted with permission from *Annals of Plastic Surgery*, 1986)

molding techniques were employed to fabricate the coupler using absorbable material polymer polyglactin which can be absorbed in 50-70 days [27]. The cut end of vessel is sent through the cuff and everted over the cuff. Then the two cuffs are connected by using the collar. There is not any foreign material in the lumen of vessels which forms a perfect intima-to-intima apposition. Figure 1.3 shows the cuffing device, including two cuffs and one collar. In 1998, a resorbable mechanical device including a cuff and a heat shrinking sleeve was brought up [35]. The smaller vessel end is sent through and everted over the cuff, then the larger vessel end is sent through the sleeve and brought over the everted smaller vessel end.

The problem with the cuffing devices is that the necessary 180°-eversion adds to the complexity and time requirement of the whole installation. Also, an assistant is needed to ensure the stabilization of the everted vessel wall on the cuff. In addition, there is a consumption of 4 mm vessels during eversion [22].

Clipping device

In 1992, a nonpenetrating method, which can be used for both end-to-end and end-to-side microvascular anastomosis, was developed by Kirsch [36]. It is called the "Vessel Closure System". Figure 1.4 shows one VCS clip. The system consists of a clip applicator, a pair of specially designed forceps for everting edges of vessels， and a clip remover [37]. With VCS clips, vessel walls are everted using forceps. Then a various number of microclips are applied. If a clip is placed wrong, a clip remover can be used to remove it easily. There are various sizes available for clips based on the thickness of the vessel wall [13]. Figure 1.5 shows the application of VCS during the creation of an

Figure 1.3. The cuffing device developed by Daniel [27]. (Reproduced with permission from *Plastic and Reconstructive Surgery*, 1984)

Figure 1.4. A VCS clip [37]. (Reproduced with permission from *The American Journal of Surgery*, 2004)

arteriovenous Brescia–Cimino fistula. The advantage of VCS is that it provides a fast and safe way to perform anastomosis and the clips do not penetrate vessel walls. The disadvantage is that it is difficult to evert the edge of vessels, especially for vessels with small diameters. A possibility of perforating walls by clips also exists.

A newer device, the U-clip device was developed by Coalescent Surgical, Inc. There are three main parts in the device: a curved suture needle at one end and a clip made of shape memory alloy nitinol at the other end and a flexible member attaching them.

Figure 1.5. Clinical use of the VCS clip applier system during the creation of an arteriovenous Brescia–Cimino fistula [37]. (Reproduced with permission from *The American Journal of Surgery*, 2004)

Figure 1.6 shows the U-clip device. With the U-clip device, once pressure is applied to a release mechanism which is located nearby the clip, the needle and the clip will be separated. Based on the property of nitinol, the clip will return to its original close-loop shape. A complete suture can be done after multiple same processes, which is similar to interrupted suture, but much faster [38]. The disadvantages of the U-clip device are that there are multiple steps needed for anastomosis, also the foreign body is exposed in the blood vessel lumen.

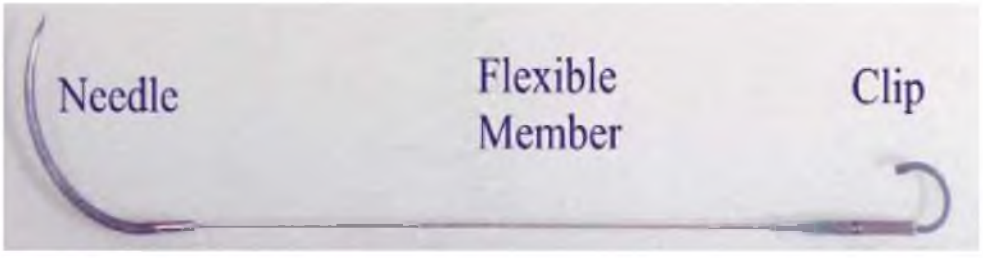

Figure 1.6. U-clip device [38]. (Reproduced with permission from *The Journal of Thoracic and Cardiovascular Surgery*, 2001)

Other devices

Ferrari developed a vascular join for end-to-end microvascular anastomosis. This device consists of two metallic rings fixed onto two polymer rings that can be connected together. As the pins just insert through the vessel wall without passing it, there is no foreign material in the lumen of the vessel [14]. Twenty end-to-end anastomoses were performed successfully in carotid arteries of sheep. Figure 1.7 shows the mechanism of the vascular joint. The problem of this device is that the elasticity property of the vessel wall will be changed due to the metal pins inside it. Also, as the thickness of vessel walls is varied, it is hard to control the metal pins inserted into the walls without penetrating the walls.

Recently a hooked device applied for smaller diameter vessel was brought up. This device is fabricated from PLGC, which is bioabsorbable. The procedure of performing vascular anastomosis is shown in Figure 1.8. First, the hooked device is placed around the vessel. Then it pierces holes on the other end of the vessel and secures the vessel on the hooks [39]. The difficulty of eversion still exists. Also suture is needed in the process of anastomosis.

Figure 1.7. Mechanism of vascular joining: the metallic pins are inserted through vessels wall with holder but do not penetrate walls [14]. (Reproduced with permission from *Interactive Cardiovascular and Thoracic Surgery*, 2007)

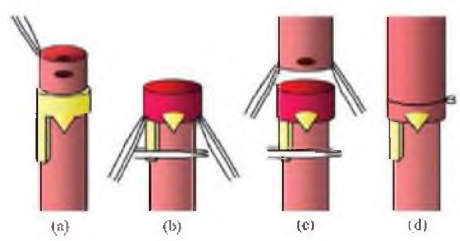

Figure 1.8. Mechanism of the bioabsorbable device with hooks [39]. (Reproduced with permission from *Microsurgery*, 2010)

A new resorbable sutureless anastomotic device was developed in 2014 [18]. This device is made from self-curing silk solution and is capable of eluting heparin once implanted. This device employs a barb-and-seat compression fitting mechanism and consists of one male and two female components. Figure 1.9 shows the working mechanism of this device. The compression mechanism determines that either it would be hard to insert the coupler into the clip or it would be too easy to pull out the assembly. The flow resistance is a limitation for this device as the implants are inserted in the vessel lumen. Also, the effects of the implants on the potential thrombosis is another concern. Table 1.1 summaries the sutureless mechanical devices for vascular anastomosis.

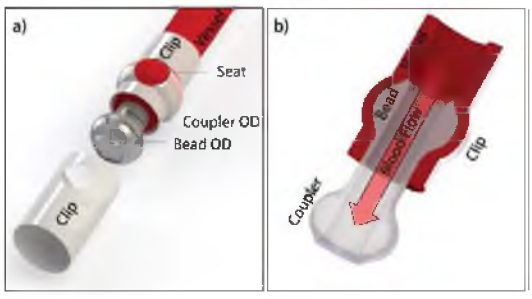

Figure 1.9. Mechanism of the resorbable barb-and-seat device [18]. (Reproduced with permission from *Journal of Biomedical Materials Research*, 2014)

Table 1.1. Mechanical Devices for Vascular Anastomosis Comparison

Technique	Researcher	Year	Material	Minimum diameter of vessel (mm)	Eversion of vessel edges (degree)
Stapler	Androsov et al. [31]	1956	Tantalum	2	180
	Inokuchi et al. [29]	1958	Tantalum	2	180
	Zingg et al. [32]	1964	Tantalum	2	180
Ring-pin	Nakayama et al. [34]	1962	Tantalum	1.5	90
	Ostrup et al. [30]	1986	polyethylene	0.8	90
Cuffing	Daniel et al. [27]	1984	polymer polyglactin	1.5	180
	Wolfgang et al. [35]	1998	poly(L-lactide-co-D, L-lactide)	1	180
Clips	Kirsch VCS [36]	1992	Titanium	2	180
	U-clip [38]	1998	Nitinol	3	/
Recent devices	Vascular join [14]	2006	Stainless steel	3	/
	Hooked device [39]	2010	PLGC	0.85	180

Non-device-based Technologies for Vascular Anastomoses

Non-device-based technologies to perform vascular anastomoses have also been developed. The most common approaches are adhesive and laser welding.

Adhesives

Adhesives have been used in tissue bonding widely in the medical field, including hemostasis, close fistulas, deliver drugs, and close cutaneous ulcers [7, 40]. Currently, there are two main groups in adhesives: fibrin glues and cyanoacrylate glues [7]. The principle of fibrin glues is the imitation of the final step of blood coagulation [41]. In 1977, Matras et al. introduced fibrin glue as a material to perform end-to-end vascular anastomosis on the carotid arteries in rats [41]. After that, Gestring et al. used fibrin glue for end-to-side vascular anastomoses in dogs and rabbits to connect a femoral artery into a femoral vein [41-43]. However, there are not long-term results for these sutureless procedures. The limitations of fibrin glues are that they may narrow the vessel lumen and affect the blood flow. Concerns about intraluminal thrombosis also exist [13, 44]. For cyanoacrylate glues, Gottlob et al. used alkyl-cyanoacrylates for vascular anastomosis by securing bushing in 1968. Short-term patency rate was achieved, but at the same time they found histotoxicity for this type of cyanoacrylate [41, 45]. Following studies also noticed the toxicity of cyanoacrylate glues. In addition, the effects of cyanoacrylate glues on the vessel walls, including giant cell formation, vessel wall thinning, elastic lamina splitting, and media calcification have also been confirmed and reported in these studies [41, 46, 47].

Overall, the amount of adhesives is essential and needs to be evaluated for different

vessel wall thickness. Also, the vessel ends need to be adjusted before application to avoid exposing the vessel lumen to the glues. These disadvantages of adhesives especially the toxicity largely limit the application of glues in clinical use.

Laser welding

Laser welding has become an alternative approach for vascular anastomosis for the past two decades. Different laser systems have been used and the following three are the main types of laser system that demonstrate effectiveness. The first type of laser is a neodymium yttrium–aluminum–garnet laser. In 1979, Jain and Gorisch first employed a neodymium yttrium–aluminum–garnet laser to perform vascular anastomosis in rat vessels without extra sutures [7]. Several years later, end-to-side anastomoses were performed on five patients with the same technique. The anastomotic procedures were done in a limited time and the patency rates were still acceptable after several months [41]. The second type of laser is an argon laser. In 1981, Gomes et al. performed a series of anastomoses on larger vessels with 4-5 mm diameters [48]. Later, White et al. used an argon laser to perform a series of artery-vein anastomoses in a clinical application and also achieved good results [49, 50]. The third type of laser is a carbon dioxide laser. With three sutures' support, both Serure et al. and Quigley et al. reported the application of a carbon dioxide laser on vascular anastomosis [51-53]. However, anastomotic aneurysm formation largely limited the success of the procedure. Around the same time, Guo et al. and Chao et al. obtained promising results using similar techniques on end-to-end anastomosis without the assistance of sutures [41, 54]. Another group also reported the application of the carbon dioxide laser welding on the

artery-vein anastomosis with supporting sutures.

Overall, the laser welding technique for vascular anastomosis has achieved certain success. However, the disadvantages of laser welding cannot be neglected. The setting of the laser power and other parameters has to be adjusted for different sizes of vessels and there has not been a certain rule reported regarding this relationship. The clinical application has only been shown on cerebral vascular anastomosis [41]. Taking the high cost of equipment and special training required for surgeons into consideration, laser welding still has a long way to go for broader clinical application.

Sutureless Anastomoses in Clinical Application

Researchers have explored various devices and methods to perform better microvascular anastomosis. A lot of experiments with some of the devices have been done on vessels in human body. Clinical application review will be focused on the UNILINK coupler and VCS clip since the two devices are widely used for anastomosis studies.

The ideal microvascular anastomosis uses less operative time and has reliable anastomosis results including a good patency rate and anastomotic strength. For the UNILINK coupler, as early as it was brought up in 1986, it attracted a lot of attention from the field of clinical application because of its faster and easier anastomosis. The patency rate has been demonstrated as good as traditional suture anastomosis. The strength of anastomosis was tested and compared to suture anastomosis. The result shows that UNILINK coupler anastomosis is even stronger than that of suture anastomosis [55]. For VCS clips, there are also numerous reviews showing that it

provides a faster and safe way for both end-to-end and end-to-side anastomosis [13]. Table 1.2 summarizes some clinical application with UNILINK coupler and VCS clips.

Motivation and Prior Design

Both UNILINK coupler and VCS clips have been used in a variety of clinical scenarios, as listed in Table 1.2. The UNILINK coupler has superior tensile strength and requires less operating time compared to the VCS. However, as the most promising method so far, the UNILINK coupler has not been able to satisfy surgeons' needs in the past few decades due to the cumbersome eversion process and the inability to work for

Table 1.2. Clinical Applications of UNILINK Coupler and VCS Clips

Devices	Researcher	Type of vessels	Number of anastomoses	Failure rate	Average anastomosis time
UNILINK coupler	DeLacure et al. [56]	arteries and veins	37	5%	5 min
	Ahn et al. [57]	arteries and veins	123	1.60%	4 min
	Nishimoto et al. [58]	veins	121	0	< 5min
	Zeebregts et al. [55]	veins	161	5%	9 min
	Jandali et al. [59]	veins	1000	0.6%	3 min
VCS clips	Cope et al. [60]	arteries and veins	153	0	not mentioned
	Zeebregts et al. [55]	arteries and veins	110	2%	17 min
	Rozen et al. [61]	arteries and veins	400	5%	15 min

both arteries and veins, which have also been discussed in the "Mechanical Devices for Vascular Anastomosis" section of Chapter 1. Improvements or new methods are needed in order to reduce operating time and technical demand, and at the same time to improve the quality of anastomosis.

Four years ago, the Gale and Agarwal labs worked together with a senior design team in the Department of Mechanical Engineering at the University of Utah to design a coupler with five rotatable wings for use with both arteries and veins. Figure 1.10 shows the device. The five wings are attached to the ring base by a plastic hinge. The wings can rotate 45° to aid spikes pressing into the vessel wall, which is supposed to simplify the eversion process of the vessel end. One drawback with the five wing coupler is that penetration of the vessel wall with the angled spikes is not consistent, thus requiring extra manual manipulation of the vessel walls over the spikes [62]. Cody Gehrke completed his MS Thesis on this device [63] and I assisted him in converting the thesis to a journal paper [62]. This design was the initial reference point for this dissertation.

The study in this dissertation aims at developing a set of vascular coupling system that can perform end-to-end anastomosis for both arteries and veins. The vascular coupling system should be efficient and easy to use. In addition, the ideal vascular coupling device should have minimum foreign materials exposed in the vessel lumen. Finally, the anastomoses should demonstrate superior leak proof abilities and withstand certain tensile force in human body.

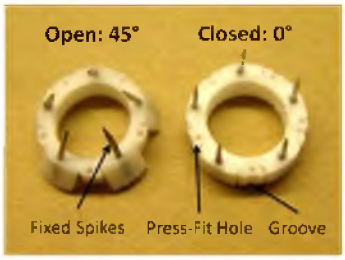

Figure 1.10. Five wing coupler [62]. (Reprinted with permission from *Biomedical Microdevices*, 2014)

Chapter Outlines

In this dissertation, the development and testing of two vascular coupling devices designed to achieve quick, efficient, and reliable end-to-end vascular anastomosis is reported. The vascular coupling devices are designed specifically to efficiently connect veins and smaller arteries found in reconstructive surgeries. The vascular coupling devices will allow surgeons to quickly reattach vessels in a safe and convenient manner. The method that has been developed reduces the amount of time in the operating room, can be done by less skilled hands, and works for both types of vessels. The details of these devices are reported as follows:

Chapter 2 introduces an enhanced ring-pin device design for both vein and artery application. This enhanced ring-pin device consists of 6 rotatable wings with a pin that slides through each wing to penetrate the vessel wall. In addition, a finite element model is built to simulate the vessel-device interaction during anastomosis and optimize the design parameters, including the number of pins, the wing pivot point, and the pin offset.

Chapter 3 introduces the fabrication, testing, and vessel strain analysis on the optimal design achieved from Chapter 2. Prototypes are manufactured using

polytetrafluoroethylene (PTFE) and high-density polyethylene (HDPE). In addition, a set of installation tools is developed to facilitate the anastomosis process. Proof-of-concept testing with the vascular coupler using plastic tubes and porcine cadaver vessels are performed to evaluate that the properties of the coupler, including the joint strength, leak resistance, and effects on flow. A simplified finite element model is assisted in the evaluation of the tearing likelihood of human vessels during installation of the coupler.

Chapter 4 develops a metal-free vascular coupling system that can be used for both arteries and veins. A set of corresponding instruments are also developed to facilitate the anastomosis process. Scanning Electron Microscopy (SEM) and Magnetic Resonance Imaging (MRI) are used to demonstrate that the anastomosis process will not cause damage on the vessel wall. Mechanical tests and cadaver animal studies are performed to show that the vascular coupling system should work as designed.

Chapter 5 introduces an initial live animal study. The vascular coupling system developed in Chapter 4 is used to perform two anastomoses on the carotid artery with PTFE graft. Ultrasound and MRI are employed to evaluate the vessel lumen and blood flow after the surgery.

Chapter 6 provides a conclusion for the dissertation highlighting the knowledge gained from the project, scientific and technological contributions, and areas where further research can be meaningfully pursued.

References

[1] K.-P. Chang, S.-D. Lin, and C.-S. Lai, "Clinical Experience of a Microvascular Venous Coupler Device in Free Tissue Transfers," The Kaohsiung Journal of Medical Sciences, vol. 23, pp. 566-572, 2007.

[2] A. S. o. P. Surgeons, "2013 Complete Plastic Surgery Statistics Report," 2013.

[3] J. W. SMITH, "Microsurgery: Review of the Literature and Discussion of Microtechniques," Plastic and Reconstructive Surgery, vol. 37, pp. 227-245, 1966.

[4] T. L. Hartzell, P. Benhaim, J. E. Imbriglia, J. T. Shores, R. J. Goitz, M. Balk, S. Mitchell, R. Rubinstein, V. S. Gorantla, S. Schneeberger, G. Brandacher, W. P. Andrew Lee, and K. K. Azari, "Surgical and Technical Aspects of Hand Transplantation: Is it Just Another Replant?," Hand Clinics, vol. 27, pp. 521-530, 2011.

[5] C. P. D. N. V. P. R. D. H. S. U. K. Shindo Ml, "USe of a mechanical microvascular anastomotic device in head and neck free tissue transfer," Archives of Otolaryngology—Head & Neck Surgery, vol. 122, pp. 529-532, 1996.

[6] C. J. Y. S. J. Ross Da and et al., "Arterial coupling for microvascular free tissue transfer in head and neck reconstruction," Archives of Otolaryngology—Head & Neck Surgery, vol. 131, pp. 891-895, 2005.

[7] P. M. N. Werker and M. Kon, "Review of facilitated approaches to vascular anastomosis surgery," The Annals of Thoracic Surgery, vol. 63, pp. S122-S127, 1997.

[8] D. Carrel, "Operative Technic of Vascular Anastomoses and Visceral Transplantation," Lyon Med, vol. 212, pp. 1561-8, 1964.

[9] H. E. M. D. Kleinert and M. L. M. D. Kasdan, "Restoration of blood flow in upper extremity injuries," Journal of Trauma-Injury Infection & Critical Care, vol. 3, pp. 461-476, 1963.

[10] H. J. Buncke and W. P. Schulz, "Total ear reimplantation in the rabbit utilising microminiature vascular anastomoses," Plastic & Reconstructive Surgery, vol. 38, p. 173, 1966.

[11] C. JR., "Free digital transfer. Report of a case of transfer of a great toe to replace an amputated thumb," J Bone Joint Surg Br, vol. 51, pp. 677-679, 1969.

[12] M. S. Alghoul, C. R. Gordon, R. Yetman, G. M. Buncke, M. Siemionow, A. M. Afifi, and W. K. Moon, "From simple interrupted to complex spiral: A systematic review of various suture techniques for microvascular anastomoses," Microsurgery, vol. 31, pp. 72-80, 2011.

[13] G. F. Pratt, W. M. Rozen, A. Westwood, A. Hancock, D. Chubb, M. W. Ashton, and I. S. Whitaker, "Technology-assisted and sutureless microvascular anastomoses: Evidence for current techniques," Microsurgery, vol. 32, pp. 68-76, 2012.

[14] E. Ferrari, P. Tozzi, and L. K. von Segesser, "The Vascular Join: a new sutureless

anastomotic device to perform end-to-end anastomosis. Preliminary results in an animal model," Interactive CardioVascular and Thoracic Surgery, vol. 6, pp. 5-8, February 1, 2007 2007.

[15] G. G. Hallock and D. C. Rice, "Early experience with the new 'megacoupler' ring-pins for microvascular anastomoses," Journal of Plastic, Reconstructive & Aesthetic Surgery, vol. 61, pp. 974-976, 2008.

[16] K. Yajima, Y. Yamamoto, K. Nohira, Y. Shintomi, P. N. Blondeel, M. Sekido, W. Mol, M. Ueda, and T. Sugihara, "A new technique of microvascular suturing: the chopstick rest technique," British Journal of Plastic Surgery, vol. 57, pp. 567-571, 2004.

[17] N. S. Levine, "Book Review," New England Journal of Medicine, vol. 299, pp. 495-495, 1978.

[18] R. R. Jose, W. K. Raja, A. M. S. Ibrahim, P. G. L. Koolen, K. Kim, A. Abdurrob, J. A. Kluge, S. J. Lin, and D. L. Kaplan, "Rapid prototyped sutureless anastomosis device from self-curing silk bio-ink," Journal of Biomedical Materials Research Part B: Applied Biomaterials, pp. n/a-n/a, 2014.

[19] A. Beris, M. Lykissas, A. Korompilias, G. Mitsionis, M. Vekris, and I. Kostas-Agnantis, "Digit and hand replantation," Archives of Orthopaedic and Trauma Surgery, vol. 130, pp. 1141-1147, 2010/09/01 2010.

[20] J. J. Disa, P. G. Cordeiro, and D. A. Hidalgo, "Efficacy of Conventional Monitoring Techniques in Free Tissue Transfer: An 11-Year Experience in 750 Consecutive Cases," Plastic and Reconstructive Surgery, vol. 104, pp. 97-101, 1999.

[21] D. T. Bui, P. G. Cordeiro, Q.-Y. Hu, J. J. Disa, A. Pusic, and B. J. Mehrara, "Free Flap Reexploration: Indications, Treatment, and Outcomes in 1193 Free Flaps," Plastic and Reconstructive Surgery, vol. 119, pp. 2092-2100, 2007.

[22] P. Tozzi, A. F. Corno, and L. K. von Segesser, "Sutureless coronary anastomoses: revival of old concepts," European Journal of Cardio-Thoracic Surgery, vol. 22, pp. 565-570, October 1, 2002 2002.

[23] A. R., "The surgery of the hand," N Y Med J, p. 59:33, 1894.

[24] N. M., "Kongress in Moskau.," Centralbl Chir, p. 24:1042, 1897.

[25] S. Lee, L. Wong, M. J. Orloff, and A. M. Nahum, "A review of vascular anastomosis with mechanical aids and nonsuture techniques," Head & Neck Surgery, vol. 3, pp. 58-65, 1980.

[26] P. E., "Beitrage zur Technique der Blutgefass-und Nervennaht nebst Mittheilungen uber die Verwendung eines resorbirbaren Metalles in de

Chirurgie," Arch Klein Chir, p. 62:67, 1900.

[27] R. K. M. D. Daniel, D. M. D. Lidman, M. M. D. Olding, J. A. P. D. D. V. M. Williams, and B. F. B. S. Matlaga, "An Anastomotic Device for Microvascular Surgery: Evolution," Annals of Plastic Surgery, vol. 13, pp. 402-411, 1984.

[28] M. D. Steven G. Friedman, "Early vascular repairs and anastomoses," in A History of Vascular Surgery, 2005, p. Page 17.

[29] K. Inokuchi, "Stapling device for end-to-side anastomosis of blood vessel," Archives of Surgery, vol. 82, pp. 337-341, 1961.

[30] L. T. M. D. Ostrup and A. M. D. Berggren, "The UNILINK Instrument System for Fast and Safe Microvascular Anastomosis," Annals of Plastic Surgery, vol. 17, pp. 521-525, 1986.

[31] P. I. Androsov, "New method of surgical treatment of blood vessel lesions," Archives of Surgery, vol. 73, pp. 902-910, 1956.

[32] W. Z. a. M. Khodadadeh, "Vascular Anastomosis—Sutures, Staples or Glue?," Can Med Assoc J, vol. 91, pp. 791-794, 1964.

[33] P. I. Androsov and F. H. Ellis, "New method of surgical treatment of blood vessel lesions," Microsurgery, vol. 13, pp. 119-125, 1992.

[34] K. Nakayama, K. Yamamoto, and T. Tamiya, "A new simple apparatus for anastomosis of small vessels. Preliminary report," J Int Coll Surg, vol. 38, pp. 12-26, 1962.

[35] R. R. Wolfgang Bähr, Ralf Gutwald, Christian Scholz, "Vascular anastomosis using a biodegradable device with a heat-shrinking sleeve: A preliminary report," Journal of Oral and Maxillofacial Surgery, vol. 56, p. 6, 1998.

[36] W. M. Kirsch, Y. H. Zhu, R. A. Hardesty, and R. Chapolini, "A new method for microvascular anastomosis: report of experimental and clinical research," Am Surg, vol. 58, pp. 722-7, 1992.

[37] C. J. Zeebregts, W. M. Kirsch, J. J. van den Dungen, Y. H. Zhu, and R. van Schilfgaarde, "Five years' world experience with nonpenetrating clips for vascular anastomoses," The American Journal of Surgery, vol. 187, pp. 751-760, 2004.

[38] A. C. Hill, T. P. Maroney, and R. Virmani, "Facilitated coronary anastomosis using a nitinol U-Clip device: bovine model," J Thorac Cardiovasc Surg, vol. 121, pp. 859-70, 2001.

[39] K. Ueda, T. Mukai, S. Ichinose, Y. Koyama, and K. Takakuda, "Bioabsorbable device for small-caliber vessel anastomosis," Microsurgery, vol. 30, pp. 494-501,

2010.

[40] R. Lerner and N. S. Binur, "Current status of surgical adhesives," Journal of Surgical Research, vol. 48, pp. 165-181, 1990.

[41] C. J. Zeebregts, R. H. Heijmen, J. J. van den Dungen, and R. van Schilfgaarde, "Non-suture methods of vascular anastomosis," British Journal of Surgery, vol. 90, pp. 261-271, 2003.

[42] L. R. Gestring GF, "Autologous fibrinogen for tissue-adhesion, hemostasis and embolization," Vasc Surg, vol. 17, p. 9, 1983.

[43] L. R. Gestring GF, Requena R, "The sutureless microanastomosis," Vasc Surg, vol. 17, p. 4, 1983.

[44] C. A. Marek, L. R. J. Amiss, R. F. Morgan, W. D. Spotnitz, and D. B. Drake, "Acute Thrombogenic Effects of Fibrin Sealant on Microvascular Anastomoses in a Rat Model," Annals of Plastic Surgery, vol. 41, pp. 415-419, 1998.

[45] B. G. Gottlob R, "Anastomoses of small arteries and veins by means of bushings and adhesive," J Cardiovasc Surg (Torino), vol. 9, p. 5, 1968.

[46] M. D. Reuben Hoppenstein, Dov Weissberg, M.D. and Robert H. Goetz, M.D., F.A.C.S., "Fusiform Dilatation and Thrombosis of Arteries Following the Application of Methyl 2-Cyanoacrylate (Eastman 910 Monomer)," Journal of Neurosurgery, vol. 23, p. 9, 1965.

[47] R. H. Goetz, D. Weissberg, and R. Hoppenstein, "Vascular Necrosis Caused by Application of Methyl 2-Cyanoacrylate (Eastman 910 Monomer): 7-Month Follow Up in Dogs," Annals of Surgery, vol. 163, pp. 242-248, 1966.

[48] M. R. Gomes OM1, Armelin E, Ribeiro M M, Brum JM, Bittencourt D, Verginelli G, Zerbini EJ., "Vascular anastomosis by argon laser beam," Tex Heart Inst J., vol. 10, p. 5, 1983.

[49] R. A. White, G. H. White, R. M. Fujitani, J. W. Vlasak, C. E. Donayre, G. E. Kopchok, and S.-K. Peng, "Initial human evaluation of argon laser—assisted vascular anastomoses," Journal of Vascular Surgery, vol. 9, pp. 542-547, 1989.

[50] R. A. White and G. E. Kopchok, "Argon laser vascular tissue fusion: current status and future perspectives," 1991, pp. 103-110.

[51] W. E. Serure A, Thomsen S, Morris J, "Comparison of carbon dioxide laser-assisted microvascular anastomosis and conventional microvascular sutured anastomosis," Surg Forum, vol. 34, p. 3, 1983.

[52] B. J. Quigley MR, Kwaan HC, Cerullo LJ, "Laser-assisted vascular anastomosis," Lancet, vol. 1985, 1985.

[53] M. R. Quigley, J. E. Bailes, H. C. Kwaan, L. J. Cerullo, J. T. Brown, C. Lastre, and D. Monma, "Microvascular anastomosis using the milliwatt CO2 laser," Lasers in Surgery and Medicine, vol. 5, pp. 357-365, 1985.

[54] J. Guo and Y. Du Chao, "Low Power CO2 Laser-assisted Microvascular Anastomosis: An Experimental Study," Neurosurgery, vol. 22, pp. 540-543, 1988.

[55] C. Zeebregts, R. Acosta, L. Bolander, R. van Schilfgaarde, and O. Jakobsson, "Clinical experience with non-penetrating vascular clips in free-flap reconstructions," Br J Plast Surg, vol. 55, pp. 105-10, 2002.

[56] M. D. DeLacure, R. S. Wong, B. L. Markowitz, M. R. Kobayashi, C. Y. Ahn, D. P. Shedd, A. L. Spies, T. R. Loree, and W. W. Shaw, "Clinical experience with a microvascular anastomotic device in head and neck reconstruction," Am J Surg, vol. 170, pp. 521-3, 1995.

[57] C. Y. Ahn, W. W. Shaw, S. Berns, and B. L. Markowitz, "Clinical experience with the 3M microvascular coupling anastomotic device in 100 free-tissue transfers," Plast Reconstr Surg, vol. 93, pp. 1481-4, 1994.

[58] S. Nishimoto, H. Hikasa, N. Ichino, T. Kurita, and K. Yoshino, "Venous anastomoses with a microvascular anastomotic device in head and neck reconstruction," J Reconstr Microsurg, vol. 16, pp. 553-6, 2000.

[59] S. Jandali, L. C. Wu, S. J. Vega, S. J. Kovach, and J. M. Serletti, "1000 consecutive venous anastomoses using the microvascular anastomotic coupler in breast reconstruction," Plast Reconstr Surg, vol. 125, pp. 792-8, 2010.

[60] C. Cope, K. Lee, H. Stern, and D. Pennington, "Use of the vascular closure staple clip applier for microvascular anastomosis in free-flap surgery," Plast Reconstr Surg, vol. 106, pp. 107-10, 2000.

[61] W. M. Rozen, I. S. Whitaker, and R. Acosta, "Venous coupler for free-flap anastomosis: outcomes of 1,000 cases," Anticancer Res, vol. 30, pp. 1293-4, 2010.

[62] C. Gehrke, H. Li, H. Sant, B. Gale, and J. Agarwal, "Design, fabrication and testing of a novel vascular coupling device," Biomedical Microdevices, vol. 16, pp. 173-180, 2014/02/01 2014.

[63] C. Gehrke, "Methods, devices, and apparatus for performing a vascular anastomosis," 2012.

CHAPTER 2

OPTIMIZATION AND EVALUATION OF A VASCULAR COUPLING DEVICE FOR END-TO-END ANASTOMOSIS: A FINITE ELEMENT ANALYSIS

Abstract

Currently, end-to-end anastomosis of blood vessels is performed using suturing, which is time consuming, expensive, and subject to large degrees of human error. One promising alternative is a ring-pin coupling device. This device has been shown to be useful for venous anastomosis, but lacks the versatility necessary for arterial applications. The purpose of this study was to optimize a vascular coupling design that could be used for arteries and veins of various sizes. To achieve this, finite element analysis was used to simulate the vessel-device interaction during anastomosis. Parametric simulations were performed to optimize the number of pins, the wing pivot point, and the pin offset of the design. The interaction of the coupler with various blood vessel sizes was also evaluated. Maximum strain in the vessel wall increased with the number of pins. The positions of the wings and pins were also important in dictating maximum strain, and improper dimensions led to failure of the installation process. Extra force applied to the distal end of the vessel, or a supplementary tool, will be required during the coupler installation process to prevent vessels less than 3 mm inner diameter (0.5 mm wall thickness) from slipping off the coupler.

Introduction

Currently, the most common technique in microsurgical vascular anastomosis involves hand suturing two cut ends of an artery or vein together with the assistance of an operating microscope. This technique is time consuming (20-40 minutes/vessel), expensive when considering doctor and operating room time, requires special training, and is subject to a great degree of human error [22]. To improve the efficiency of the anastomotic operation processes, a series of innovative methods have been investigated, including metallic staple devices, cuffing rings, clips, adhesives, and laser welding [1, 3, 4, 6, 8, 9, 10, 16, 18, 20]. The potential of these approaches has been limited due to the lack of biocompatibility, complex procedures for use, and general inefficiency.

The most successful attempt at simplifying the manual suturing technique has been seen with a device consisting of a polymer ring with fixed pins perpendicular to the ring over which the vessel walls are everted, and which will be referred to as a "ring-pin" device in this paper. Nakayama designed the first ring-pin device in 1962 [14]. The device consisted of a metal ring, on which there were 6 pins and 6 pinholes evenly spaced. Unlike staple devices requiring blood vessels to be everted 180°, a 90° vessel end eversion is sufficient for ring-pin devices. The most popular ring-pin device is a commercially available venous coupling device from Synovis [15]. This device is made of a rigid high density polyethylene (HDPE) ring on which there are six pins and six pinholes. The devices are anchored to the blood vessel ends and are then brought together to re-establish the continuity of the blood vessel. The ring-pin devices work well for veins, but are not as effective with arteries due to the increased wall thickness, elasticity, and intraluminal pressure of arteries compared to veins. Attempts at using

ring-pin devices for arteries requires extra vessel securing steps, such as with elastic bands [17], which undesirably adds time and complexity, largely negating the benefits of the device over traditional manual suturing. A vascular coupling device with five wings that everts the vessel 45° was developed to solve this problem [5], but the 45° angled pins do not penetrate the vessel wall smoothly and consistently. Thus, there is still a need for a better vascular coupling device for use with both veins and arteries.

Here we present an enhanced ring-pin device design consisting of 6 wings with a pin that slides through each wing to penetrate the vessel wall (Figure 2.1). The wings are attached to a ring base with plastic hinges that allow the wings to rotate from 0° to 90°, and serve to open and close the coupling device. The ring base has six evenly spaced holes that receive the corresponding pins from a mating coupler. The anastomotic process with the enhanced coupler design can be successfully completed in four steps. First, the wings are opened 90° relative to the ring base and the pins are in a fully retracted position (Figure 2.1(a)). The free end of the blood vessel is slid through the coupler. Second, the pins are pushed towards the center of the coupler and the vessel wall is penetrated by the pins (Figure 2.1(b)). Third, the wings are closed by rotating the pins 90° from the initial state, stretching the vessel open to expose the intima (Figure 2.1(c)). Finally, the two couplers, one for each end of the mating vessels, are joined by inserting the pins from one coupler into the corresponding holes of the complementary coupler. This results in an intima-to-intima connection of the blood vessel.

The critical step in the anastomosis process is the third step when the pins are rotated 90° and the vessel end is stretched open. The vessel can slide off from the pins or be damaged by the stretching process. Either outcome would be considered a failure

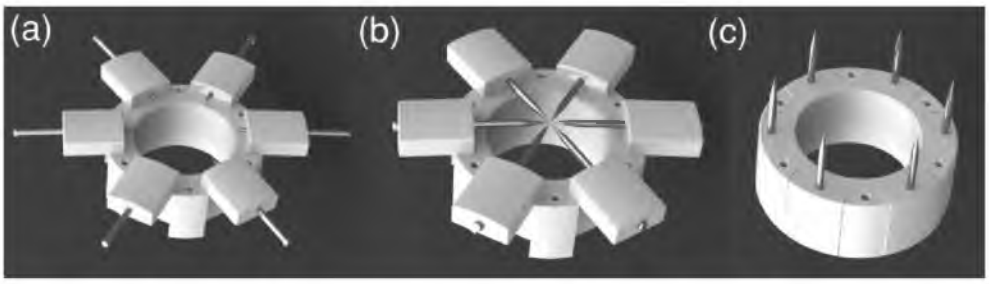

Fig 2.1 The working mechanism of the vascular coupler: (a) Image showing the vascular coupler in its starting configuration. The free end of a blood vessel is slid through the center of the ring. (b) The six pins are then pushed towards the center of the coupler to penetrate the vessel wall. (c) The wings and pins are rotated 90° to open the vessel and couple with the free end of the mating vessel, which is attached to a second coupler.

of the anastomosis procedure. The objective of this study was to determine the optimal features for the enhanced ring-pin design that would result in consistent and complete vessel end stretching with low strain in the vessel wall, and to ensure the functionality of the coupler with blood vessels of varying dimensions. While experimental evaluation is a valuable step in the design process [13], finite element modeling (FEM) offers a unique and inexpensive method to study the physics of the device without a large number of manufacturing steps or physical experiments. It has been successfully used in many medical device studies, including those for splint design, dental implantation, and locking compression plate optimization [2, 7, 12]. FEM has also been widely employed for device-artery interaction simulations, including stent design [19]. Therefore, in this study, we developed a FE model to simulate the third step of the anastomosis procedure. We then use the model to identify the ideal number of pins, the wing pivot point , and the pin offset to minimize strain in the vessel wall while still resulting in a complete

end-to-end anastomosis. We also evaluated how varying vessel diameter and size affected the successful completion of the anastomosis with the coupler.

Materials and Methods

Finite Element Model Development

Base model geometry

The base design for the model was the enhanced ring-pin device containing 6 wings and pins (Figure 2.2(a)). To minimize computational time, the three-dimensional FE model took advantage of the radially symmetric geometry and properties of the blood vessel and the simultaneous movement of the 6 wings and pins of the coupler. Therefore, only 1/6 of the vessel and coupler was modeled, as shown in Figure 2.2. The blood vessel had a 5 mm outer diameter, 4 mm inner diameter, and a length of 15 mm. The diameter dimensions were estimated from blood vessel measurements made in our lab. The length of the blood vessel was estimated from the space where a clamp would be applied at approximately this position during surgery, according to a skilled surgeon (co-author; JA). The plastic wings around the pins were not included in the model as their main function is to provide a channel through which the pins slide and rotate. The wings do not interact with the blood vessel directly. The pin length in the model was set to 3 mm, which represents the length of the pin left outside of the wing after being pushed towards the center. The distance from the outer diameter of the vessel to the end of the pin (distance between line 2 and 3 in Figure 2.2(c)) was termed the wing pivot dimension.

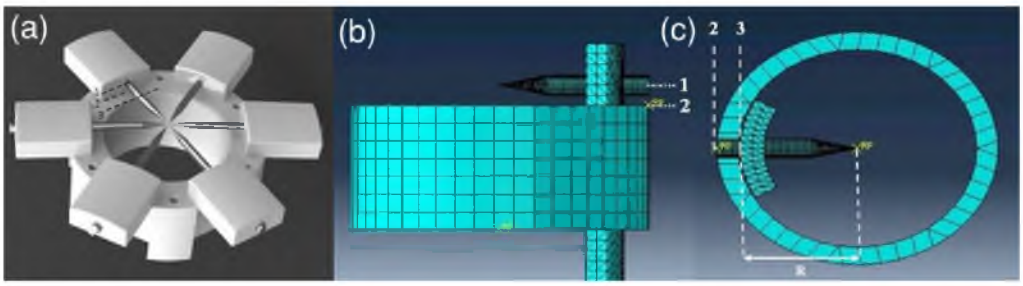

Fig 2.2 The coupler model: (a) The coupler model in SolidWorks. (b) The pin offset was defined as the distance between the pin center (line 1) and the top edge of the ring base (line 2). (c) The wing pivot dimension was defined as the distance between the distal edge of the pin (line 2) and the inner diameter edge of the ring base (line 3).

Theoretically, only 1/6 of the ring base was required for the model; however, for visualization purposes, the entire ring base was included in the model. The ring base had a 6 mm outer diameter, a 5 mm inner diameter, and a height of 3 mm. The pin was placed 1 mm below the free end of the vessel. The ring base was placed outside the blood vessel and 0.5 mm below the center of the pin end (distance between line 1 and 2 in Figure 2.2(b)). This distance was termed the pin offset. The model geometry was created in SolidWorks (2012×64 Edition, Dassault Systems SolidWorks Corp) and imported into ABAQUS CAE (6.11-2, Dassault Systems) for meshing and analysis.

Meshing

The blood vessel was meshed with linear tetrahedral elements. The pin and ring base were represented as rigid bodies because of their comparatively small deformation to the blood vessel. A convergence study on the vessel wall was performed to ensure the answer converged to a stable solution. Mesh quality was also evaluated. The final number of elements in each mesh of the base model was 18827, 2360, and 703 for the

vessel, pin, and ring base, respectively. The same average edge length was used to mesh vessels with increased or decreased dimensions from the base model.

Material properties

The blood vessel was assumed to be an isotropic hyperelastic material that can be represented by a form of the polynomial strain energy potential, which has been found to adequately describe the nonlinear relationship of arteries [11]:

$$U=C_{10}(I_1-3)+C_{01}(I_2-3)+C_{20}(I_1-3)^2+C_{11}(I_1-3)(I_2-3)+C_{02}(I_2-3)^3 \qquad (1)$$

where U is the strain energy density function of the hyperelastic material, C_{ij} are temperature-dependent hyperelastic constants, and I_1 and I_2 are the strain invariants. The material parameters for the blood vessel were obtained from experimental data for human femoral arteries, in which mass density is 1050 kg/m^3, C_{10} is 18.9 kPa, C_{02} is 2.75 kPa, C_{20} is 85.72 kPa, C_{11} is 590.43 kPa, and C_{02} is 0 kPa [11]. This material model was verified by creating a separate FE model of just the vessel and simulating tensile tests reported in the literature [21]. Stress-strain data in the simulations were compared to those reported in the experiments. All simulations resulted in $< 3\%$ difference from the published values (data not shown) and the vessel material model was therefore determined to be an appropriate representation of the vessel.

Boundary conditions, pin rotation, and contact interactions

Because only 1/6 of the vessel was modeled, radially symmetric boundary conditions were applied to the lateral free edges. The distal 'clamped' end of the blood

vessel had all degrees of freedom fully restrained. A rotation center, located at the wing pivot point, was created 0.5 mm below the center of the pin based on the geometric design of the coupler. A 180°/s counterclockwise angular velocity was applied to the pin which rotated it around this rotation center. The total length of time that the pin was rotated was 0.5 s, which resulted in a complete 90° rotation of the pin. The ring base had all degrees of freedom fully constrained (no motion allowed) and acted as a barrier for blood vessel motion, which was representative of its interaction with the vessel during an actual anastomosis procedure. The contact interaction between the blood vessel, the pin, and the ring base were all assumed to be frictionless based on experimental observations of minimal adhesion between the vessel and the coupler [13]. During post-processing, the maximum logarithmic strain in the vessel was evaluated as well as a successful 90° reflection of the vessel wall.

Design variables

In the design optimization process, three main design variables were investigated to determine the optimal features of the coupler. The first variable was the number of pins on the coupler. The second and third variables investigated were the pin offset and the wing pivot dimension, respectively.

Number of pins

The base model for the coupler included six pins and wings as this is the design of the Synovis ring-pin couplers. The ideal pin number causes minimal strain in the vessel wall during the stretching process and ensures a full 90° eversion of the vessel, which

generates in an intima-to-intima connection. To discover the optimal pin number for the coupler, the number of pins (three, four, five, six, eight, and ten) were varied, and both theoretical and finite element (FE) analyses were employed to predict the maximum strain in the vessel wall during the stretching process (Table 2.1).

In the theoretical analysis, the blood vessel was simplified to a 2D circle before stretching, with a 5 mm outer and a 4 mm inner diameter. During the stretching process, the pins rotate 90° around the wing pivot point. As the number of pins, n, increases, the vessel forms a polygon with n sides. The distance between the center of the blood vessel and the center of the pin end was 3.75 mm in the base model (n=6), which was the radius of the circumcircle of the polygon. The strain was calculated based on the change in the perimeter from the unstretched circle to the stretched polygon. In the FE analysis, six models were created. Each model contained a unique number of pins, n, which resulted in only $1/n$ of the vessel being represented. For example, in the base model, six pins were included. The radially symmetric nature of the problem resulted in only 1/6 of the vessel wall needing to be represented. During the stretching process of

Table 2.1. Configurations of stretched vessels for theoretical and FE analysis

3	4	5	6	8	10
					
	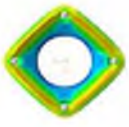	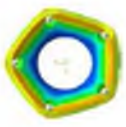	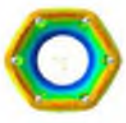	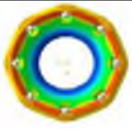	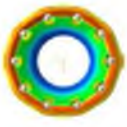

each model simulation, the maximum logarithmic strain in the vessel wall was recorded. Once an optimal number of pins was determined, the bending moment applied to those pins during the procedure was evaluated. This was done by checking the reaction moment created at the wing pivot point. This moment was used to analyze the degree of pin bending and evaluate the possibility of the pin being misaligned with the hole in the mating coupler.

Positions of wings and pins

In addition to the number of pins, the wing pivot point dimension and the pin offset of the coupler have an effect on the rotation of the pins, which will ultimately affect strain of the blood vessel. Intuitively, the larger the two variables are, the more the vessel end will be stretched and increase vessel strain. Thus, we typically would like to minimize these values. However, minimizing the values means minimizing the ring base and wing thickness. This could increase the potential for damage during manufacturing and handling, and could significantly influence the tolerances required for the design.

In this study, we opted to see how large we could make the wing pivot dimension and pin offset before failure of the vessel occurs. Therefore, two series of parametric simulations were performed. The first series of simulations varied the wing pivot dimension from 0.5-1.0 mm in increments of 0.1 mm and kept the pin offset at a constant value of 0.5 mm. The second series of simulations varied pin offset values 0.5-1.0 mm in increments of 0.1 mm and kept the wing pivot dimension at a constant value of 0.5 mm. Both series of simulations were performed on the model with optimal pin

numbers. The vessel failure was defined with a logarithmic strain threshold of 1.05, which is the reported ultimate strain of femoral arteries for people 20 to 29 years old [21].

Application to blood vessels with different geometries

Average dimensions of arterial vessels measured in our lab were approximately 5 mm outer and 4 mm inner diameter. However, in reality, vessel size will vary depending on vessel type. We plan to design several sized coupler devices to encompass a range of vessel types. However, it is unclear if the mechanics and interaction of the system with the vessel will remain constant at different scales. To evaluate the feasibility or challenges of using scaled coupler designs on smaller vessels, and to discover if the stretching process could still be completed without tearing the vessel, two couplers and blood vessels with smaller dimensions were modeled.

The dimensions of the cross sections, the length of the pins, and the size of the coupler rings for the two scaled models are given in Table 2.2. The length of the blood vessels were kept at 15 mm. The wing pivot dimension and the pin offset were kept the same as the base model (0.5 mm). The length of the pin was defined by the outer radius of the blood vessel plus the wing pivot dimension. For example, the length of pins in the base model (3 mm) equals 2.5 mm (half OD) plus 0.5 mm.

Table 2.2. Geometry modification on the smaller vessel models

Model	Cross section		Length of pins	Coupler ring	
	OD(mm)	ID(mm)	(mm)	OD (mm)	ID(mm)
Base Model	5	4	3	6	5
Medium Vessel	4	3	2.5	5	4
Small Vessel	3	2	2	4	3

Results

Based on the experimental observations in our lab, the finite element model of the coupler and vessel successfully captured the qualitative deformation of the vessel during the third step of the anastomosis procedure when the wing motion was applied (Figure 2.3). That is, as the pin rotated, the blood vessel stretched radially as well as along the vessel axis. For visualization purposes, an entire vessel is shown in Figure 2.3(a) by axisymmetrically replicating the pattern of strain from the ¼ vessel model. In each simulation, the maximum principle strain was located around the hole made by the pin and distributed out in a butterfly shape.

Number of pins

From the theoretical analysis, it can be seen that increasing the number of pins increased the perimeter of the final stretched polygon, suggesting that strain in the

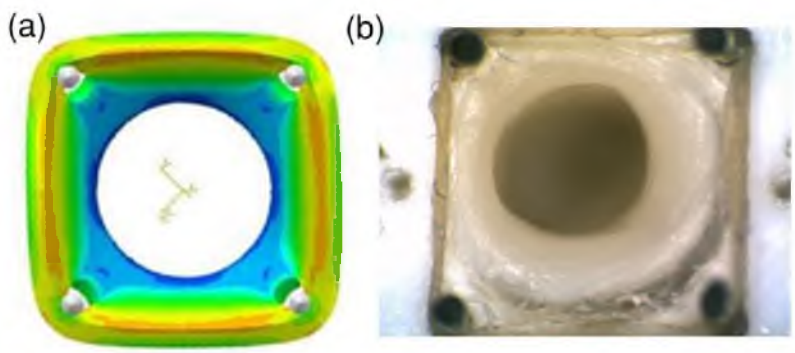

Fig 2.3. Comparison between the FE model and the bench testing: (a) The FE model of the coupling device with four pins; (b) A porcine artery stretched open with a four-pin coupling device.

vessel end would also increase with the number of pins. This was corroborated with the FE analysis as maximum strain increased with an increase in the number of pins (Figure 2.4). The differences of the maximum strain results between theoretical and finite element analyses were due to the model simplification for the theoretical analysis. The vessel-pin interaction and the pierced holes in the vessel wall led to strain redistribution and stress concentrations when compared to an idealized vessel. For the theoretical analysis, the maximum strain calculation was fully based on the geometric change of the vessel end. Therefore, the strain results showed a clear increase with an increase in pin number. However, for the finite element analysis, the maximum strain was found around the pierced holes, so the effect of the final stretched vessel configuration on the maximum strain was not as significant as for the theoretical analysis.

For both analyses, the coupler with three pins resulted in a triangular configuration when the vessel end was completely stretched open (90° rotation). The triangular edges of this configuration cut across the lumen of the coupler and were not able to cover the entire ring base, as shown in the Table 2.2. The incomplete coverage might cause the

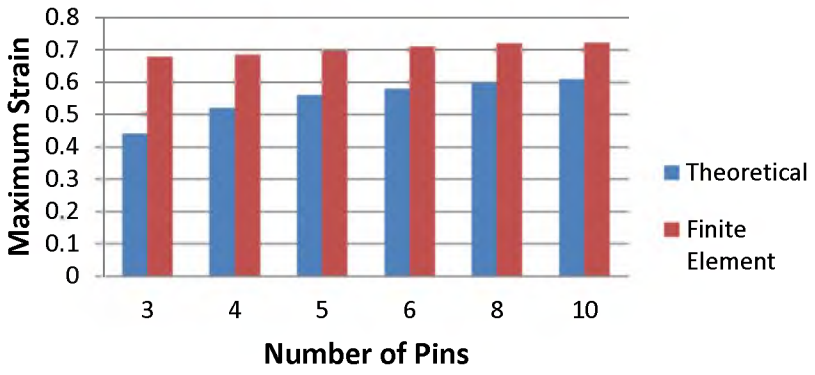

Fig 2.4. The maximum strain in the vessel wall during the stretching process for different numbers of pins.

edges of the blood vessel to collapse inside the lumen of the vessel when connecting with the mating coupler, which could damage the vessel or lead to the coupler material being exposed to the intima of the vessel and the blood. All other pin variations resulted in a complete exposure of the lumen of the vessel and would appear to result in a successful intima-to-intima connection of the vessel. For these reasons, the coupler with four pins was selected as the optimal design. It resulted in a maximum strain in the vessel wall that was 35% lower than the ultimate strain of femoral arteries.

For a four-pin design, the maximum bending moment required to rotate the pin to completely stretch the vessel was found to be 1.12 N-mm. The deflection or bending of the pin caused by this moment was calculated to be 0.009 mm based on a stainless steel material for the pin. This deflection was 1.8% of the diameter of a pin hole along the ring base. Even with this deflection, the sharpened pin head would still be able to enter the pin hole on the mating coupler. Any small deflection, such as this, would likely correct itself as the pin body is slid into the hole. Thus, any risk of coupler mismatch would be minimal with this four-pin design.

Positions of wings and pins

Modifying the wing pivot point and the pin offset of the coupler resulted in a noticeable change in the maximum strain of the vessel wall. The maximum vessel strain increased with increases in the wing pivot point while the pin offset was kept constant (Figure 2.5). Specifically, the maximum strain in the vessel wall changed from 0.68 to 0.80 as the wing pivot point was increased from 0.5 to 1.0 mm. Despite this change, all of the maximum strain values were 35% to 23% lower than the ultimate strain of human femoral arteries, suggesting that any of these pivot dimensions would be acceptable. When pin offset was varied and the wing pivot point was held constant, the maximum strain in the vessel wall increased with the pin offset for the first four positions and then decreased with the pin offset for the last two positions (Figure 2.5). The reason for the change in trend was because the vessel began to slip off of the pins at pin offsets > 0.7 mm. The vessel completely slipped off the pin with a 1.0 mm pin offset.

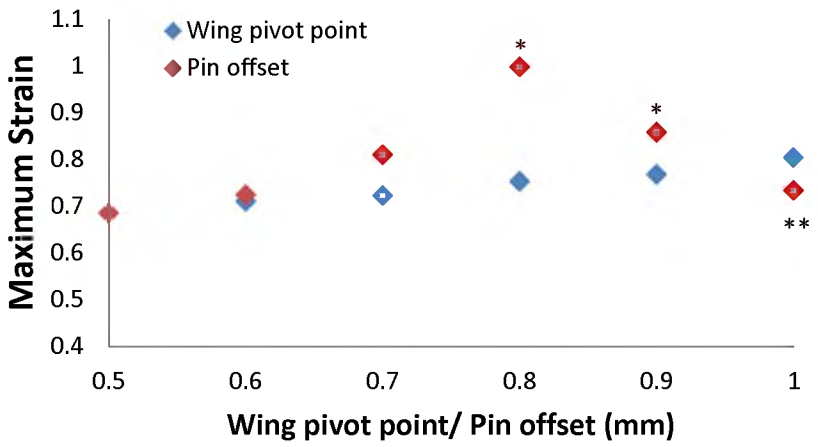

Fig 2.5. The maximum strain in the vessel wall increases with the wing pivot point location (blue). The maximum strain in the vessel wall first increases with the pin offset (red) and then decreases due to the vessel end slipping off from the pins. *vessel began to slip off the pin. **vessel completely slipped of the pin.

Application to blood vessels with different geometries

Simulations with smaller vessels and the scaled couplers resulted primarily in the vessel slipping off the pins, as shown in Figure 2.6. For visualization purposes, an entire vessel is shown in Figure 2.6 by axisymmetrically replicating the pattern of strain from the ¼ vessel model. The same wing pivot point and pin offset resulted in the same difference between the radius of the circumcircle of the polygon, R, and the radius of the vessel, r, regardless of blood vessel geometry ($\Delta r = R - r = 1$ mm). In the theoretical analysis, the expression of the stretching ratio for the four-pin coupler is $(4\sqrt{2}R - 2\pi r)/(2\pi r)$. Thus, the stretching ratio of smaller vessels will be higher compared to larger vessels, resulting in the vessels slipping off of the pin during the stretching process.

In an effort to keep the vessel end on the pins with the smaller couplers during the whole stretching process, an external force was applied at the distal vessel end to help pull the vessel onto the pins and overcome the retraction force. For the medium vessel size with 4 mm outer and 3 mm inner diameters, it was found that 0.4 N was sufficient to keep the vessel on the pins during the stretching process. For the small vessel size with 3 mm outer and 2 mm inner diameters, it was found that 0.8 N was required to keep the vessel on the pins. The 0.4 N force for the medium coupler/vessel resulted in a maximum strain that was still 20% lower than the ultimate strain of the vessel wall. However, the 0.8 N force required for the smallest coupler/vessel resulted in a maximum vessel wall strain that was 95% greater than the defined strain failure threshold, which meant the vessel would likely tear in this scenario. For smaller coupler designs, it will likely be necessary to have a supplementary tool to prevent the vessel

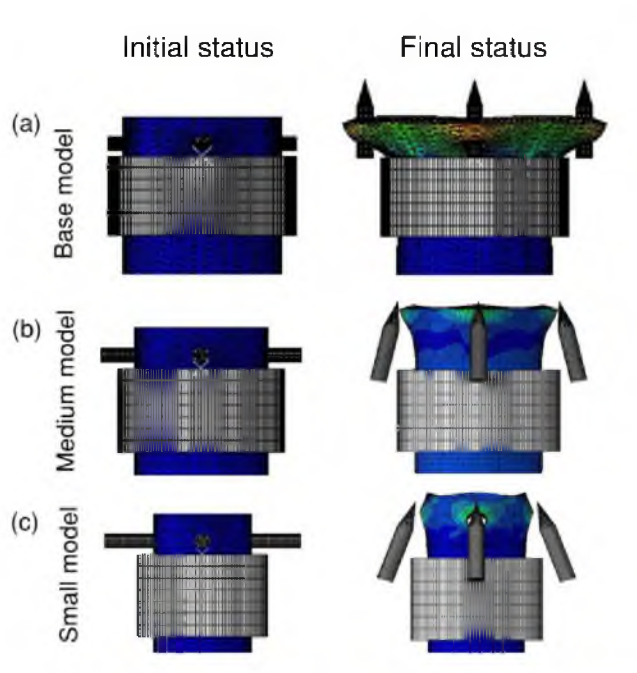

Fig 2.6. Vessel deformation at the initial and final status for the (a) base blood vessel model with 5 mm outer and 4 mm inner diameter; (b) medium blood vessel model with 4 mm outer and 3 mm inner diameter; (c) small blood vessel model with 3 mm outer and 2 mm inner diameter.

end from slipping off of the pins. Coating the pins in order to increase the friction between the pin and the vessel wall is also a possible solution.

Discussion

This study provides a new design for both artery and vein anastomosis. The design variables of the coupler have direct impact on the performance of the proposed coupler design and are evaluated with FE methods. The number of pins and the positions of wings and pins are optimized to achieve the lower strain in the vessel wall, the easier alignment, and the successful vessel eversion. This information is not only valuable for a better understanding of the device mechanism, but also very helpful when considering

future manufacturing and designs. The models of blood vessels with smaller dimensions provide guidance for the future scaling of this device to handle vessels of differing sizes.

This study contains several assumptions and limitations. First, the material properties of the artery wall are assumed to be isotropic hyperelastic. In reality, an artery has a three-layer structure and is anisotropic. These variables will have an influence on the strain distribution in the vessel wall. However, published literature shows that a isotropic hyperelastic material can adequately represent the nonlinear properties of the vessel wall. In addition, a separate arterial tension simulation has been performed to verify the material model. Second, the variations of the vessel properties are not considered for different artery types and sizes. These variations will lead to different absolute values for the results, but may have small effects on the qualitative trend and optimization analysis. Third, the artery model is represented as an ideal cylinder. In the real scenario, the artery will not be fully axisymmetric and the movement of the coupler wings might not be simultaneous, so the 1/n simplification will not be appropriate. However, for an initial optimization study, considering the comparative nature for different design variables, the above simplification is acceptable. Fourth, in the validation study, the maximum strain is not measured in the experimental test. The qualitative result shows the vessel deformation when closing the coupler wings. Finally, vessel failure is defined as the reported ultimate strain of femoral arteries for people 20 to 29 years old. For older people, the average ultimate strain is around 0.87, which is lower for younger people. However, the maximum strain in the vessel wall during the stretching process with the coupler is still below the ultimate strain and the optimization results are not affected.

Conclusion

A new ring-pin coupling device with rotatable wings and translatable pins was designed and optimized. The optimal pin number and the geometric features of the coupler design were studied by numerical simulation. A coupler with four pins was selected as the optimal design due to the lower strain of the vessel wall during the stretching process, the convenience of installation and alignment, and the ability to provide an intima-to-intima anastomosis. The geometric features of the coupler, such as the wing pivot point and pin offset, significantly increased the vessel strain and/or vessel slipping during the installation process and should be minimized as much as possible. The scaled coupler designs for blood vessels with different geometries clearly illustrated that merely scaling down the device will not be sufficient. Additional force, tools, or friction between the pin and the vessel wall will be required for successful intima-to-intima anastomosis. In summary, the results of this work have led to an optimal ring-pin coupler design, and provided insight into the tools or modifications that will be required to install the coupler on vessels of multiple sizes.

References

[1] Andel CJ, Pistecky PV, and Borst C (2003) Mechanical properties of porcine and human arteries: implications for coronary anastomotic connectors. *Ann Thorac Surg* 76: 58-64.

[2] Chang CL, Chen CS, Huang CH, and Hsu ML (2012) Finite element analysis of the dental implantation using a topology optimization method. Med Eng Phys 34: 999-1008.

[3] Ferrari E, Tozzi P, and von Segesser LK (2007) The vascular join: a new sutureless anastomotic device to perform end-to-end anastomosis. Preliminary results in an animal model. Interact Cardiovasc Thorac Surg 6: 5-8.

[4] Filsoufi FR, Farivar S, Aklog L, Anderson CA, Chen RH, Lichtenstein S, Zhang J, and Adams DH (2004) Automated distal coronary bypass with a novel magnetic coupler (MVP system). J Thorac Cardiovasc Surg 127: 185-192.

[5] Gehrke C, Li H, Sant H, Gale B, and Agarwal J (2014) Design, fabrication and testing of a novel vascular coupling device. Biomed Microdevices 16: 173-180.

[6] Gummert JF, Opfermann U, Jacobs S, Walther T, Kempfert J, Mohr FW, and Falk V (2007) Anastomotic devices for coronary artery bypass grafting: technological options and potential pitfalls. Comput Biol Med 37: 1384-1393.

[7] Huang TH, Feng CK, Gung YW, Tsai MW, Chen CS, Liu CL (2006) Optimization design of thumbspica splint using finite element method. Med Bio Eng Comput 44:1105-1111.

[8] Jacobs S, Mohr FW, and Falk V (2004) Facilitated endoscopic beating heart coronary bypass grafting using distal anastomotic device. Int. Congr Ser 1268: 809-812.

[9] Klima U, Maringka M, Bagaev E, Kirschner S and Haverich A (2004) Total magnetic vascular coupling for arterial revascularization. J Thorac Cardiovasc Surg 127: 602-603.

[10] Lally C, Reid AJ, and Prendergast PJ (2004) Elastic behavior of porcine coronary artery tissue under uniaxial and equibiaxial tension. Ann Biomed Eng 32: 1355-1364.

[11] Lally C, Dolan F, and Prendergast PJ (2005) Cardiovascular stent design and vessel stresses: a finite element analysis. J Biomech 38: 1574-1581.

[12] Lee CH, Shih KS, Hsu CC, Cho T (2014) Simulation-based particle swarm optimization and mechanical validation of screw position and number for the fixation stability of a femoral locking compression plate. Med Eng Phys 36: 57-64.

[13] Li H, Gehrke C, Gale BK, Sant H, Coats B, Agarwal J (2015) A New Vascular Coupler Design for End-to-End Anastomosis: Fabrication and Proof-of-Concept Evaluation. J. Med. Devices doi: 10.1115/1.4029924

[14] Nakayama K, Yamamoto K, and Tamiya T (1962) A new simple apparatus for anastomosis of small vessels. Preliminary report. J Int Coll Surg 38:12-26.

[15] Ross DA, Chow JY, Shin J, and Restifo R (2005) Arterial coupling for microvascular free tissue transfer in head and neck reconstruction. Arch Otolaryngol Head Neck Surg 131: 891-895.

[16] Scheltes JS, van Andel CJ, Pistecky PV, and Borst C (2003) Coronary anastomotic devices: blood-exposed non-intimal surface and coronary wall stress. J Thorac Cardiovasc Surg 126: 191-199.

[17] Spector JA, Draper LB, Levine JP, and Ahn CY (2006) Routine use of microvascular coupling device for arterial anastomosis in breast reconstruction. Ann Plast Surg 56: 365-368.

[18] Suyker WJ, Buijsrogge MP, Suyker PT, Verlaan CW, Borst C, and Grundeman PF (2004) Stapled coronary anastomosis with minimal intraluminal artifact: The S2

Anastomotic System in the off-pump porcine model. J Thorac Cardiovasc Surg 127: 498-503.

[19] Timmins LH, Moreno MR, Meyer CA, Criscione JC, Rachev A, Moore Jr JE (2007) Stented artery biomechanics and device design optimization. Med Bio Eng Comput 45: 505-513.

[20] Ueda K, Mukai T, Ichinose S, Koyama Y, and Takakuda K (2010) Bioabsorbable device for small-caliber vessel anastomosis. Microsurgery 30: 494-501.

[21] Yamada H and Evans FG (1970) Strength of Biological Materials. Baltimore: Williams & Wilkins.

[22] Zdolsek J, Ledin H, Lidman D (2005) Are mechanical microvascular anastomoses easier to learn than suture anastomoses?. Microsurgery 25: 596-598

CHAPTER 3

A NEW VASCULAR COUPLER DESIGN FOR END-TO-END ANASTOMOSIS: FABRICATION AND PROOF-OF-CONCEPT EVALUATION

Reprinted from Journal of Medical Devices, doi: 10.1115/1.4029924

Journal of Medical Devices. Received July 07, 2014;
Accepted manuscript posted March 2, 2015. doi:10.1115/1.4029924

A New Vascular Coupler Design for End-to-End Anastomosis: Fabrication and Proof-of-Concept Evaluation

Huizhong Li[1], Cody Gehrke[1], Bruce K. Gale[1], Himanshu Sant[1], Brittany Coats[1] and Jay Agarwal[2]

(1) Department of Mechanical Engineering, University of Utah, Salt Lake City

(2) Department of Surgery, University of Utah, Salt Lake City

Bruce K. Gale (Corresponding author)
Email: bruce.gale@utah.edu
Phone: (801)585-5944
Address: 50 S Central Campus Drive Rm 2110, Salt Lake City, UT 84112

Abstract— Traditional hand-suturing for vascular connection techniques are time consuming, expensive, and require highly complex instruments and technical expertise. The aim of this study is to develop a new vascular coupler that can be used in end-to-end anastomosis surgery in an easier and more efficient way for both arteries and veins. The vascular coupler has four rotatable wings and one translatable spike in each wing. Prototypes were manufactured using polytetrafluoroethylene (PTFE) and high-density polyethylene (HDPE). A set of installation tools was designed to facilitate the anastomosis process. Proof-of-concept testing with the vascular coupler using plastic tubes and porcine cadaver vessels showed that the coupler should work as designed. A simplified finite element model assisted in the evaluation of the tearing likelihood of human vessels during installation of the coupler. Results of tests on the coupler showed that the vascular coupler could be efficiently attached to blood vessels, did not leak after the anastomosis was performed, had sufficient joint strength, and had little impact on flow in the vessel. The entire anastomosis process can be completed in three minutes when using the vascular coupler to join porcine cadaver vessels.

Keywords: Vascular coupler, anastomosis, medical device, finite element analysis.

1. INTRODUCTION

During the past decades, microsurgery has brought great change to the field of reconstructive surgery for both research and clinical application [1]. Common microsurgical procedures are replantation and free tissue transfer, during which blood vessels in the donor tissue are cut and then reattached during tissue reconstruction [2]. Success in both replantation and free tissue transfer requires instant survival and long term function [3]. Failure can result in flap necrosis and wound breakdown, which are harmful and life threatening [2].

The standard technique for performing microvascular anastomosis was developed in 1902 [4]. When Jules Jacobson carried out the first microvascular surgery, the penetrating suture with attached needles became the gold standard for microvascular anastomosis [5]. As surgical expectations become more and more challenging, the limitations of standard vascular anastomosis, which is time consuming, highly expensive and requires technical expertise and complex lab instruments, have hindered the productivity and

Journal of Medical Devices. Received July 07, 2014;
Accepted manuscript posted March 2, 2015. doi:10.1115/1.4029924

effectiveness of surgeons. Sutures can lead to a variety of problems and errors can even lead to suspension of the surgery [6]. Even if everything goes well, it takes approximately 30 minutes for a skilled surgeon to complete one anastomosis in the operating room. For a replantation or free tissue transfer surgery, where multiple vessels need to be reconnected, hand suturing is very time consuming and subject to a great degree of human error [7].

There have been several attempts to improve the efficiency of the anastomosis operation process and reduce the impact of surgical dexterity on anastomosis outcomes [8], [9], [10], [11], [12], [13], [14], [15], [16], [17]. These attempts were either more cumbersome than traditional hand suturing, unable to maintain a tight seal, or increased thrombosis rates. One device, called the "GEM Microvascular Anastomotic Coupler" (Synovis Micro, Birmingham, AL), consists of two coupling rings with six fixed pins [2]. This device is commonly applied to veins but does not work effectively on arteries. It can be difficult to stretch the artery to hook it onto the pins manually. Also, arteries tend to slip off the pins during the installation process because of the elasticity and the thickness of the arterial wall. Alternative methods, like adding rubber bands to secure arteries on the pins, have been employed, but they often add to the complexity of using the GEM coupler during surgery [18]. This problem has been partially solved by a vascular coupling device (VCD) with five wings that can rotate 45° [19]. The wings allow the spikes to be pressed through the vessel wall at an angle of 45°, which simplifies the mounting of the VCD onto the vessel compared to existing devices without wings. One drawback with the VCD is that the angled spikes do not always "catch" the vessel walls, and when they do, the vessel walls do not always slide down the spikes as needed, thus requiring manual manipulation of the vessel walls over the spikes. A higher angle of incidence would improve the penetration of the spikes and ensure full penetration of the spikes.

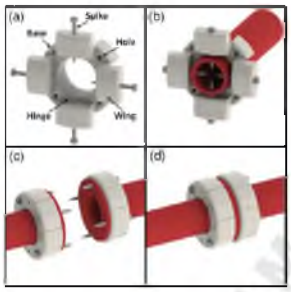

Fig. 1. Image showing the coupler design and overview of the operation of the vascular coupler: (a) Basic coupler design. (b) Punctured vessel. (c) Wings folded back with the couplers ready to be joined. (d) Coupled vessel.

Accordingly, we propose a new vascular coupler (Fig. 1) with four rotatable wings and four translatable spikes,. It can be used not only on veins but also on arteries. The movability of the wings and pins enable the coupler to be mounted on arteries and makes the process simple and convenient. A set of installation tools has also been developed to facilitate the anastomosis process. A series of proof-of-concept evaluations have been performed to estimate the functionality of the vascular coupler.

2. Materials And Methods

2.1 Vascular coupler design and fabrication

Fig 1(a) shows the design of the vascular coupler. The coupler has a ring-shaped base with a smooth inner surface, through which the severed end of a blood vessel can pass. Four wings are attached to the ring base by plastic living hinges, which allow rotation of the wings from 0° to 90°. Four spikes are inserted into the

Journal of Medical Devices. Received July 07, 2014;
Accepted manuscript posted March 2, 2015. doi:10.1115/1.4029924

four wings and can translate through the wings. There are four holes evenly spaced on the ring base for receiving the spikes from a mating coupler.

The entire anastomosis process can be successfully completed in four steps (Fig 1(b)-(c)): First, one end of the blood vessel passes through the coupler and four stainless steel spikes slide towards the center of the blood vessel and penetrate through the vessel wall. Second, the four wings of the coupler close by rotating 90° from the initial state, placing all of the spikes in a parallel configuration. During the wing rotation, the end of the blood vessel stretches open. The same procedure is performed on the opposite blood vessel with another coupler. Finally, the two couplers and their vessel ends are connected together by inserting the spikes of one coupler into the corresponding holes of the opposing coupler. Once the two couplers are connected, the intima of the two vessels are automatically aligned and pressed to each other. The friction force between the spikes and holes provides a good bond, producing an intima-to-intima anastomosis. This configuration ensures the blood flow will not be exposed to foreign material and largely reduces the risk of thrombosis [20]. In addition, the couplers can reduce the chance of vessel collapse or contraction by physically keeping the vessel open at the point of coupling.

The main body of the couplers has been made of either polytetrafluoroethylene (PTFE) or high density polyethylene (HDPE), which are both biocompatible materials. The spikes are made of stainless steel. PTFE was selected because of its compatibility with laser machining, which can be used for fast prototyping in the design optimization process. HDPE was used for manufacturing the finalized couplers due to its superior mechanical properties, including its appropriate hardness and easy fabrication.

The PTFE couplers were cut with a CO_2 laser using two drawing layers. One layer was a through cut and the other layer was a blind cut, which creates the hinges for the wings. The first step is to cut out four blind lines from a PTFE sheet, which is securely mounted in the laser bed by tape. The second step is to cut through lines required to separate the coupler from the material sheet and spike holes. The HDPE couplers were fabricated using a traditional manufacturing method. First, the HDPE ring and spike holes are machined with a CNC. The wings are cut using a razor blade positioned in a custom jig shown in Fig 2(b) and (c). Fig 2(b) shows a through cut to cut one side of a wing. Four cuts are made in this position after rotating the ring a ¼ turn. Four similar cuts are performed with the ring at the top location of the jig. Fig 2(c) shows a blind cut to produce the wing hinge.

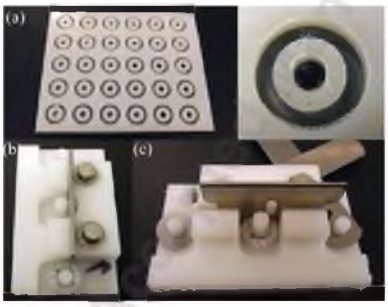

Fig. 2. HDPE coupler manufacturing process: (a) Inner circle, outer circle and spike holes are machined using a CNC. (b) The through side cuts of the wing are made. (c) The blind center cuts of the wing are made.

2.2 Installation tool

A set of tools were designed and fabricated to facilitate the anastomosis process, including translation of the four spikes and rotation of the four wings. The set consists of six tools: right and left base tools, a cam

Journal of Medical Devices. Received July 07, 2014;
Accepted manuscript posted March 2, 2015. doi:10.1115/1.4029924

tool, an anvil tool, and right and left wing closure tools, as shown in Fig 3. Each tool was created to perform a specific role in the anastomosis, which can be described as follows.

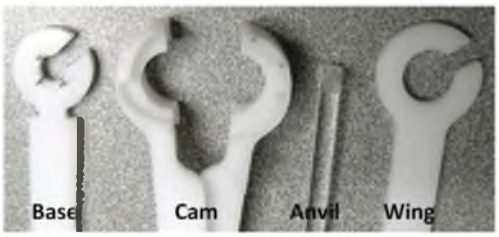

Fig. 3. The cam tool set showing the right base, cam, anvil, and wing closure tools.

The function of the base tool is to hold the coupler and provide the foundation for all of the other tools during installation. It holds the coupler in place with three small pillars that are pressed into the back of the coupler. The blood vessel is allowed to pass through the coupler when it is mounted on the base tool. The cutout section on the base tool allows the coupled vessel to be removed when the anastomosis is complete.

The cam tool uses four cams to press the spikes through the vessel wall at a 90° angle. This step is performed by opening up the cam-head like a pair of pliers and then closing around the circular head on the base tool and the attached coupler. The cam tool fits around the base tool, and the base tool provides the axis of rotation for the cam tool. The spikes are then pushed towards the center of the coupler by rotating the cam tool 90° relative to the base tool. The cam tool also supports the wings and keeps them perpendicular to the vessel wall. Once the cam tool has been rotated and the spikes have penetrated the vessel wall, the cam tool is removed by simply opening the handles.

The anvil tool is used to prevent the collapse of the vessel wall while the spikes are being pressed through the vessel. The head of the anvil tool is a cylinder that is about the same diameter as the inner diameter of the vessel. The cylinder has grooves cut out of it that allow the spikes to penetrate through the vessel and into the anvil.

The wing closure tool performs the function of pressing down the wings. The inner diameter of the tool head is the same size as the diameter of the coupler. The inner ring of the wing closure tool has a slight chamfer which helps center the tool on the coupler. Once centered, the tool is simply pressed on the coupler. This step rotates the wings to the closed position and secures them until the connection with the other vessel is completed and the tool is removed.

2.3 Proof-of-concept testing

A series of bench tests were performed to demonstrate the functionality of the couplers, including a separation test to determine how much force the interface between the two couplers can withstand, a leakage test, and a flow test to determine the couplers' effects on the flow.

For the separation test, small diameter wires were placed around each of the couplers and two couplers were connected. One end of the wire connecting with the upper coupler was hung from a clamp. By adding weight gradually at the other end of the wire connecting with the bottom coupler, the force required to separate the two couplers were recorded. Four pairs of both PTFE and HDPE couplers were used in this experiment. For the leakage test, two pieces of latex tubing were joined with the coupler. Latex tubing was used to simulate the artery due to its relatively similar properties and thickness of the tubing wall. One end of the latex tubing was plugged, and water was applied to the other end. Water pressure was increased slowly to an extreme (360 mmHg) value above normal blood pressure (<200 mmHg). Once there was leakage, the water pressure was recorded with a pressure gauge (WIKA Instrument, GA). For the flow test,

Journal of Medical Devices. Received July 07, 2014;
Accepted manuscript posted March 2, 2015. doi:10.1115/1.4029924

two latex tubes were connected with the HDPE coupler. Another uncut piece of latex tubing with the same length as the coupled one was prepared as a control. Water at 160 mmHg, 260 mmHg, and 360 mmHg, which corresponds to an extended range of blood pressure, was pushed through both the coupled and control tubes. The pressure before and after the couplers for each driving fluid pressure was measured three times with a pressure gauge (WKA Instrument, GA). Significant differences in pressure drop between experimental setups were determined by a Student's t-test.

2.4 *Ex vivo* testing

To evaluate the usability of the coupler on blood vessels, including the effectiveness of the installation process and the likelihood of tearing during installation of the coupler, the couplers and the installation tools were tested on two carotid arteries and two jugular veins. Both arteries and veins were harvested from cadaver pigs and tested when still fresh.

2.5 Simplified finite element model

While *ex vivo* testing on porcine vessels was designed to provide good evidence of the functionality of the couplers, but the mechanical properties of human arteries can be different. To evaluate the likelihood of a human vessel tearing during the coupler installation process, a finite element (FE) model was built to simulate the stretching process of the vessel end, as shown in Fig 4(a)-(b).

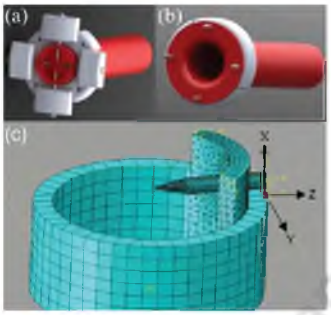

Fig. 4. Basic FEA model geometry: Image (a) shows the initial state of the four wings, Image (b) shows the final, idealized state when the four wings are closed and the end of blood vessel is stretched, Image (c) shows a ¼ radial symmetry model including one spike and the blood vessel.

The FE model consisted of the blood vessel and coupler. The wings of the coupler were excluded because they don't interact with the blood vessel until the rotation is complete. Only one spike and ¼ of the blood vessel were modeled as the coupler and blood vessel are radially symmetric. The blood vessel in the model was represented as a cylindrical vessel with 5 mm outer and 4 mm inner diameters, respectively. These dimensions are consistent with the dimensions of the arteries used in the physical experiments. The length of the blood vessel in the model was 15 mm, as it was assumed a clamp would be applied at approximately this position during surgery. The coupler ring had a 6 mm outer diameter, a 5 mm inner diameter, and a length of 3 mm. The 3 mm long spike was placed 1 mm below the cut edge of the vessel, as shown in Figure 5(c).

The blood vessel was modeled as an isotropic hyperelastic material. The form of the polynomial strain energy potential used is

$$U=C_{10}(I_1-3)+C_{01}(I_2-3)+C_{20}(I_1-3)^2+C_{11}(I_1-3)(I_2-3)+C_{02}(I_2-3)^3, \qquad (1)$$

Journal of Medical Devices. Received July 07, 2014;
Accepted manuscript posted March 2, 2015. doi:10.1115/1.4029924

where U is the strain energy density, Cij are temperature-dependent material parameters, I_1 and I_2 are the strain invariants. The material parameters for the model were obtained from experimental data for human femoral arteries [21]. To validate the material model, a separate finite element model was created to simulate tensile tests of blood vessels published in the literature (data not shown) [22]. The coupler ring and spike were modeled as rigid bodies since the deformation of the coupler ring and the spike are very small relative to the blood vessel.

The distal 'clamped' end of the blood vessel was modeled by fixing all degrees of freedom. Two radially symmetric boundary conditions were applied on the lateral cut surfaces of the vessel to account for only modeling ¼ of the vessel. The center of rotation of the spike due to the living hinge in the physical coupler is 0.5 mm below the center of the spike end. A 90° counterclockwise rotation of the spike about the y-axis (Fig. 4(c)) was applied in the model at this same center of rotation location. The contact interaction between the vessel and all components of the coupler was assumed as frictionless since the adhesion between the vessel and the coupler is minimal. The stretching ratio and logarithmic strain are commonly used to predict failure for human vessels [23]. Therefore, the locations and values of the maximum principle logarithmic strain in the model were evaluated.

3. Results

3.1 Fabrication results

Both PTFE and HDPE couplers were fabricated with laser cutting and traditional machining, respectively. Fig. 5 shows a pair of PTFE and HDPE couplers, one with spikes out and the other with spikes in.

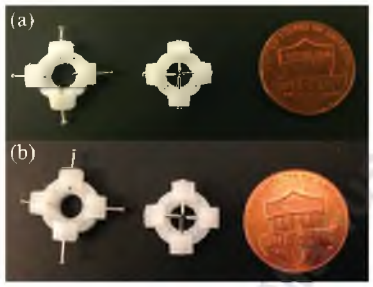

Fig. 5. Vascular couplers made of (a) PTFE and (b) HDPE: The left coupler shows the initial state before the spikes are pushed in; the right couplers shows the state after the spikes pushed in.

The installation tools were cut out of the acrylic. The application sequence for the complete tool set (Fig. 6) is as follows:

(a) The base and cam tools are handed to a surgeon as a single unit with the couplers mounted on the base tool.
(b) The blood vessel is pushed though the coupler until one-half of the vessel diameter protrudes past the face of the coupler.
(c) The anvil tool is installed by aligning its handle with the handle of the base tool and pushing the anvil into the lumen of the vessel.
(d) The cam tool is rotated clockwise 90°, which presses the spikes through the vessel wall.
(e) The cam tool is removed.
(f) The wings are depressed by pushing the wing closure tool over the coupler as it is still mounted to the base tool.

Journal of Medical Devices. Received July 07, 2014;
Accepted manuscript posted March 2, 2015. doi:10.1115/1.4029924

(g) The second coupler is installed on the opposite vessel end using the same process. Once the couplers are installed on both vessel ends, the two couplers are pressed together to form an intima-to-intima anastomosis (The vessel is removed in Fig. 4(g) to show internals).
(h) The tools are then removed and the anastomosis is complete.

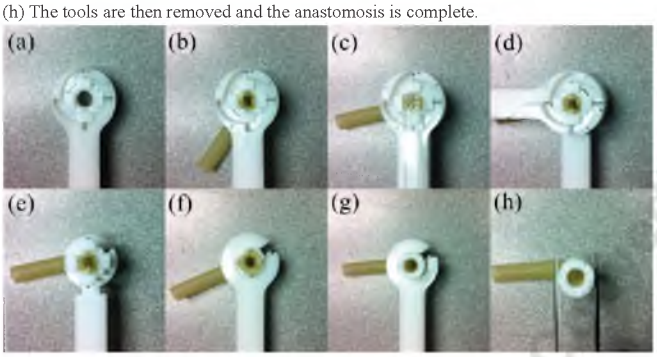

Fig. 6. Composite photo shows the steps of the coupling process.

3.2 Proof-of-concept testing results

Both PTFE and HDPE couplers were tested for the separation force. An average coupling strength resulted in 19±4 N for the PTFE couplers and 30±1 N for the HDPE couplers. For blood vessels with 5 mm outer and 3 mm inner diameters connected with couplers, the results would correspond to a vessel tensile loading of 1.5 MPa and 2.3 MPa, respectively. As the normal physiologic load for human carotid arteries is around 13.3 kPa [24], [25], both PTFE and HDPE couplers should withstand all normal loads that occur on a blood vessel in the body. The leakage tests with the HDPE couplers showed that there is no leakage associated with pressures up to the maximum applied 360 mmHg. This pressure is far above physiological conditions. The results of the flow tests are plotted in Fig. 7. The pressure drop across the coupled tubing was not significantly different from the control tubing, except at high pressures ($p=0.006$). The lower resistance to flow may be due to the coupler helping to hold open the tubing lumen.

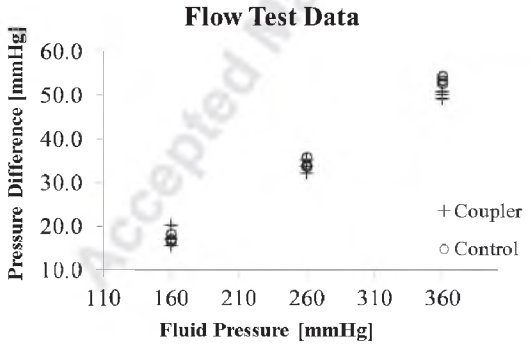

Fig. 7. Plot of the flow test data showing the relationship between pressure drop in the tubing and overall fluid pressure across the coupled and control tubing.

Journal of Medical Devices. Received July 07, 2014;
Accepted manuscript posted March 2, 2015. doi:10.1115/1.4029924

3.3 *Ex vivo* testing results

Fig. 8(a)-(d) shows the coupling process of porcine blood vessels using the vascular couplers and its tools. The entire process can be done in less than three minutes by both surgeons and engineers after basic training. Fig. 8(e) shows a porcine cadaver artery installed on one coupler. The artery is stretched open and hooked on four spikes. The lumen of the artery is completely open and the intima is smooth and ready for the connection. The 90° penetration of the spikes and the translation ability ensure the efficient and consistent anchoring process. Of the four porcine vessels tested (two arteries and two veins), there was no visible tearing of the tissue.

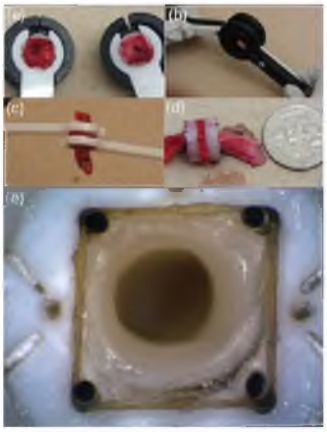

Fig. 8. Images (a)-(d) show the anastomosis process of two porcine cadaver vessels with the vascular couplers; Image (e) shows the porcine cadaver vessel being stretched by four spikes.

3.4 FEA modeling results

Fig. 9 shows modeling results for various rotation angles of the spike and the stretching effect on the vessel. With the spike rotation, the blood vessel stretches radially as well as along the vessel axis.

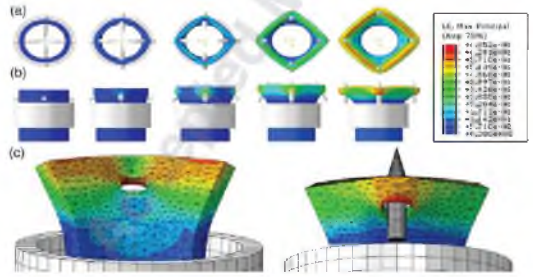

Fig. 9. Simulation result images (a) and (b) shows the top and side view of the stretching process of the vessel end; Images (c) shows the strain distribution at the vessel end.

Journal of Medical Devices. Received July 07, 2014;
Accepted manuscript posted March 2, 2015. doi:10.1115/1.4029924

The maximum principle strain was 0.685 and located around the hole and distributed out in a butterfly shape. For people 20 to 29 years old, the ultimate strain of femoral arteries is 1.05, while for older individuals it can be slightly lower [25]. Based on the model results for this configuration, the likelihood of blood vessel tearing is low. Thus, the results suggest that the coupler could be used to successfully couple arteries for most people without tearing of the vessel. Note that even if the vessel tears, the coupler can still provide a successful anastomosis as the torn region will be located near the spike placement and will be compressed between the two couplers.

4. DISCUSSION

The vascular couplers in this study not only inherit the advantages of earlier VCD, such as rapid deployment, a better seal, absence of foreign material in the lumen of the vessel, and the ability to withstand high separation forces, but they also make several improvements that result in a more efficient and convenient method for end-to-end anastomosis. First, the new design was able to reduce the number of spikes found in commercial devices from 6 to 4. This reduction will speed up the installation process and prevent delays due to misalignment. Second, the spike in previous VCD design has been limited to 45° of rotation and is not able to slide within the coupler, resulting in poor penetration of the tissue [19]. The rotation of the wings from 0 ° to 90° and the ability of the spikes to slide within the wings in the new device allows for a more efficient and robust insertion of the spikes through the blood vessels, as was illustrated in the porcine *ex vivo* testing.

Proof of concept of the usability of the couplers was demonstrated using bench tests and porcine cadaver vessels. The separation, leakage and flow bench tests of the coupler showed that the coupler outperforms the necessary requirements to withstand physiological conditions. Experiments using cadaveric vessels showed that the anastomotic process could be done quickly with the device. The geometric features of the newly developed cam tool also simplify the coupling process and ensure a better control of the individual tasks of the anastomosis. The lower technical expertise requirement could allow more surgeons to perform the anastomotic surgery and reduce the human error. In the future, couplers with various sizes (2mm, 3mm, 4mm and 5mm) will be built for different vessel sizes. For vessels whose sizes are in between these standard sizes, the larger coupler will be chosen to avoid narrowing the vessel lumen and limiting the blood flow. The possible effects on the blood flow for the small mismatch necessitate further investigation.

To validate that the coupler should work equally well in human vessels, a simplified FE model was built to estimate the performance of the coupler on human blood vessels. Results of the FE model showed that the blood vessel deformation shape after the completion of the spike's rotation were in general agreement with the *ex vivo* results. The strain distribution pattern shows that the maximum strain on the blood vessel was lower than ultimate strain reported in the literature for adults (20-29 years old). For older people, the average ultimate strain is around 0.87, which is still above the maximum strain found in the model, suggesting that the coupler could be used with a wide range of individuals. One limitation on the validation of the FE study is that the maximum strain experienced by a human femoral artery while being stretched by the coupler was not measured to validate the model results. Nevertheless, the results suggest that arteries should not tear when used in the coupler, as was shown in the porcine artery testing experiments, and thus we anticipate that the coupler will work well with human arteries.

5. CONCLUTION

In conclusion, a new vascular coupler with rotatable wings and translatable spikes and a set of installation tools specifically for end-to-end anastomosis have been successfully designed, fabricated and tested to show proof-of-concept of the design. The vascular coupler is easy to use and demonstrates zero leakage under physiological conditions, minimal to no effect of flow, and the ability to withstand high separation force. Both the modeling and the *ex vivo* testing results show that the vascular coupler could open the vessel end without damaging it. Modeling results and *ex vivo* tests suggest that the vessels should withstand

Journal of Medical Devices. Received July 07, 2014;
Accepted manuscript posted March 2, 2015. doi:10.1115/1.4029924

the forces applied by the coupler and that might be found in the body. With minimum training, the implementation of the current device requires less than three minutes to complete an end-to-end anastomosis. With further manufacturing development to allow mass production and meet appropriate regulatory guidelines, the vascular coupler will achieve its potential as an implantable end-to-end anastomosis device and make a valuable tool for the medical community.

ACKNOWLEDGEMENTS

The authors would like to acknowledge Troy Orr for his help on the HDPE coupler's fabrication and the financial support of Technology Commercialization Project, University of Utah.

REFERENCES

[1] K. P. Chang, S. D. Lin, and C. S. Lai. Clinical experience of a microvascular venous coupler device in free tissue transfers. *Kaohsiung J. Med. Sci* 2007; 23: 566-572.

[2] D. A. Ross, J. Y. Chow, J. Shin, and R. Restifo. Arterial coupling for microvascular free tissue transfer in head and neck reconstruction. *Arch Otolaryngol Head Neck Surg* 2005; 131: 891-895.

[3] R. K. Daniel, D. Lidman, M. Olding, J. A. Williams, and B. F. Matlaga. An anastomotic device for microvascular surgery. *Ann Plast Surg* 1984; 13: 402-411.

[4] D. Carrel. Operative technic of vascular anastomoses and visceral transplantation. *Lyon medical* 1964; 212: 1561-1964.

[5] H. E. Kleinert and M. L. Kasdan. Restoration of blood flow in upper extremity injuries," *J Trauma Acute Care Surg* 1963; 3: 461-476.

[6] K. Yajima, Y. Yamamoto, K. Nohira, Y. Shintomi, P. N. Blondeel, M. Sekido, W. Mol, M. Ueda, and T. Sugihara. A new technique of microvascular suturing: the chopstick rest technique. *British Journal of Plastic Surgery* 2004; 57: 567-571.

[7] J. Zdolsek, H. Ledin, D. Lidman. Are mechanical microvascular anastomoses easier to learn than suture anastomoses?. *Microsurgery* 2005; 25: 596-598.

[8] C. J. Andel, P. V. Pistecky, and C. Borst. Mechanical properties of porcine and human arteries: implications for coronary anastomotic connectors. *Ann Thorac Surg* 2003; 76: 58-64.

[9] E. Ferrari, P. Tozzi, and L. K. von Segesser. The Vascular Join: a new sutureless anastomotic device to perform end-to-end anastomosis. Preliminary results in an animal model. *Interact Cardiovasc Thorac Surg* 2007; 6: 5-8.

[10] F. R. Filsoufi, S. Farivar, L. Aklog, C. A. Anderson, R. H. Chen, S. Lichtenstein, J. Zhang, and D.H. Adams. Automated distal coronary bypass with a novel magnetic coupler (MVP system). *J Thorac Cardiovasc Surg* 2004; 127: 185-192.

[11] J. F. Gummert, U. Opfermann, S. Jacobs, T. Walther, J. Kempfert, F. W. Mohr, and V. Falk. Anastomotic devices for coronary artery bypass grafting: technological options and potential pitfalls. *Comput Biol Med* 2007; 37: 1384-1393.

[12] S. Jacobs, F. W. Mohr, and V. Falk. Facilitated endoscopic beating heart coronary bypass grafting using distal anastomotic device. *Int. Congr Ser* 2004; 1268: 809-812.

[13] U. Klima, M. Maringka, E. Bagaev, S. Kirschner and A. Haverich. Total magnetic vascular coupling for arterial revascularization. *J Thorac Cardiovasc Surg* 2004; 127: 602-603.

Journal of Medical Devices. Received July 07, 2014;
Accepted manuscript posted March 2, 2015. doi:10.1115/1.4029924

[14] C. Lally, A. J. Reid, and P. J. Prendergast. Elastic behavior of porcine coronary artery tissue under uniaxial and equibiaxial tension. *Ann Biomed Eng* 2004; 32: 1355-1364.

[15] J. S. Scheltes, C. J. van Andel, P. V. Pistecky, and C. Borst. Coronary anastomotic devices: blood-exposed non-intimal surface and coronary wall stress. *J Thorac Cardiovasc Surg* 2003; 126: 191-199.

[16] W. J. Suyker, M. P. Buijsrogge, P. T. Suyker, C. W. Verlaan, C. Borst, and P. F. Grundeman. Stapled coronary anastomosis with minimal intraluminal artifact: The S2 Anastomotic System in the off-pump porcine model. *J Thorac Cardiovasc Surg* 2004; 127: 498-503.

[17] K. Ueda, T. Mukai, S. Ichinose, Y. Koyama, and K. Takakuda. Bioabsorbable device for small-caliber vessel anastomosis. *Microsurgery* 2010; 30: 494-501.

[18] J. A. Spector, L. B. Draper, J. P. Levine, and C. Y. Ahn. Routine use of microvascular coupling device for arterial anastomosis in breast reconstruction. *Ann Plast Surg* 2006; 56: 365-368.

[19] C. Gehrke, H. Li, H. Sant, B. Gale, and J. Agarwal. Design, fabrication and testing of a novel vascular coupling device. *Biomed Microdevices* 2014; 16: 173-180.

[20] N. Chernichenko, D. A. Ross, J. Shin, J. Y. Chow, C. T. Sasaki, and S. Ariyan. Arterial coupling for microvascular free tissue transfer. *Otolaryngol Head Neck Surg* 2008; 138: 614-618.

[21] C. Lally, F. Dolan, and P. J. Prendergast. Cardiovascular stent design and vessel stresses: a finite element analysis. *J Biomech* 2005; 38: 1574-1581.

[22] H. Yamada and F. G. Evans. Strength of Biological Materials. *Baltimore: Williams & Wilkins;* 1970.

[23] B. R. Simon, M. V. Kaufmann, M. A. McAfee, and A. L. Baldwin. Finite element models for arterial wall mechanics. *J Biomech Eng* 1993; 115: 489-496.

[24] T. Khamdaeng, J. Luo, J. Vappo, P. Terdtoon, and E. E. Konofagou. Arterial stiffness identification of the human carotid artery using the stress–strain relationship in vivo. *Ultrasonics* 2012; 52: 402-411.

[25] G. Sommer, P. Regitnig, L. Költringer, and G. A. Holzapfel. Biaxial mechanical properties of intact and layer-dissected human carotid arteries at physical and supraphysical loadings. *Am. J. Physiol., Heart Circ* 2010; 298: 898–912.

CHAPTER 4

A NOVEL VASCULAR COUPLING SYSTEM FOR END-TO-END ANASTOMOSIS

Preliminary Design and Testing

Design, Fabrication, and Testing of a Novel End-to-End Vascular Coupling System

Huizhong Li, Bruce K. Gale, *IEEE Member*, Himanshu Sant, Jill Shea, Jay Agarwal

Abstract— **Microvascular anastomosis is common and necessary during reconstructive and free tissue transfer surgeries. Traditional hand suturing techniques are time consuming, subject to human error, and require complex instruments. Prior attempts including staples, ring-pin devices, cuffing devices, and clips were either more cumbersome, were unable to maintain a tight seal, or did not work for both arteries and veins. To provide a more efficient and reliable vessel anastomosis, a pin-free vascular coupling system that can be used for both arteries and veins was designed and manufactured. A set of corresponding instruments were developed to facilitate the anastomosis process. Both bench testing and *ex vivo* testing were performed to evaluate the operating abilities of the vascular coupling system. Preliminary studies were performed on cadaver pigs.**

I. Introduction

During replantation and free tissue transfer surgeries, it is often necessary to cut and reattach vessels [1]. The current state of the art in microsurgical vascular anastomosis is hand suturing the two cut ends of an artery or vein together using ultrafine techniques with the assistance of an operating microscope [2]. This technique requires specialized training, is time consuming, expensive when considering doctor and operating room time and is subject to a great degree of human error [3]. There have been many attempts to identify alternatives to the current manual suturing technique. Typical examples are staples, clips, cuffing rings, adhesives and laser welding [4,5,6,7,8,9,10,11,12,13], all of which have fallen short due to the lack of biocompatibility, complexity of design and general inefficiency.

A commercially successful approach to simplifying the manual suturing technique exists with the "GEM Microvascular Anastomotic Coupler" (Synovis Micro, Birmingham, AL) [14]. This device makes use of two high density polyethylene (HDPE) rings which are anchored to the cut ends of two veins. The two rings are then brought together to juxtapose the two cut vessel ends, thereby re-establishing the continuity of the vein. Due to the increased wall thickness, elasticity, and intraluminal pressure of arteries over veins, this device has had a limited role in successful arterial anastomosis. Attempts at using this device for arterial anastomosis have only been successful with significant modification, which undesirably adds time and complexity over traditional manual suturing. Another vascular coupling device partially solved the problem by replacing the rigid ring base with a ring having five rotating wings [15]. While this device works well for arteries, it can still require some manual manipulation of the vessel for consistent pin penetration. It is worth noting that most of the current anastomotic devices involve the eversion of the vessel end, which stretches the blood vessel wall and increases the possibility of tearing if pins are used.

The new vascular coupling system provides an easy and efficient installation process without the use of wall-penetrating pins. A set of installation instruments has been developed to facilitate the anastomosis process. Mechanical and *ex vivo* testing have been performed to estimate the functionality and feasibility of the vascular coupling system. Preliminary studies were performed on cadaver pigs.

II. Materials and Methods

A. Coupler design and fabrication

The coupler consists of an engaging ring and a back ring for each vessel end (Fig. 1). In the process of anastomosis (Fig. 2), one end of the vessel is passed through the back ring with about 2mm of vessel extending beyond the edge. The end of the vessel is then clipped (1-2mm) to allow for release of tension at the free edge and easy eversion of the vessel over the back ring. Finally the engaging ring is installed onto the back ring and a friction fit is used to engage the clipped ends of the vessels between the engaging ring and the back ring. The same installation process is performed on the opposite vessel. The two couplers installed on the vessel ends are offset 90°. When connected, the two arms on the engaging rings hook into a groove at the bottom of the opposing back ring to finally lock and secure the two vessel ends to each other.

Figure 1 (A) The engaging ring, (B) The back ring.

Research supported by TCIP from University of Utah.

H. Li is with the Department of Mechanical Engineering, University of Utah, Salt Lake City, UT 84112, USA (phone: 801-558-0839; e-mail: lizzylee2526@gmail.com).

B. Gale is with the Department of Mechanical Engineering, University of Utah, Salt Lake City, UT 84112, USA (e-mail: bruce.gale@utah.edu).

H. Sant is with the Department of Mechanical Engineering, University of Utah, Salt Lake City, UT 84112, USA (e-mail: himanshu.sant@utah.edu).

J. Shea is with the Department of Surgery, University of Utah, Salt Lake City, UT 84112, USA (e-mail: Jill.Shea@hsc.utah.edu).

J. Agarwal is with the Department of Surgery, University of Utah, Salt Lake City, UT 84132, USA (e-mail: Jay.Agarwal@hsc.utah.edu).

978-1-4244-7929-0/14/$26.00 ©2014 IEEE

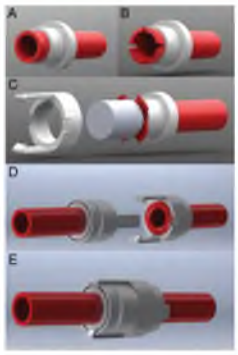

Figure 2 (A) The vessel is passed through the back ring, (B) The end of the vessel is clipped 1-2mm, (C) The vessel end is everted using the temporary placement of an anvil, (D) The engaging rings are installed on both vessel ends, (E) Two vessels are connected.

The device is designed to keep the vessels open and prevent any parts from coming in contact with blood flowing through the vessel, which not only reduces the chance of blockage or collapse at the point of coupling, but reduces the risk of thrombosis.

Coupler prototypes were fabricated and designed to establish the proof of concept. The engaging rings were built from Vero White and polylactic acid (PLA) using 3D printing techniques. Back rings were built from polymethyl methacrylate (PMMA) using laser cutting.

B. Installation apparatus

A set of instruments aimed at facilitating the anastomosis process using the coupler were designed and fabricated. The instrument set includes a holder and an anvil instrument (Fig. 3). The holder is used for holding the back ring. In the holder instrument, two anchor arms are connected using the pinned hinge at the end. The difference between the two anchors is that the heads are offset from each other by 90° to allow the two couplers held by the instruments to be locked with each other at the completion of the anastomosis process. Each anchor arm is used for one cut end of the vessel to be anastomosed.

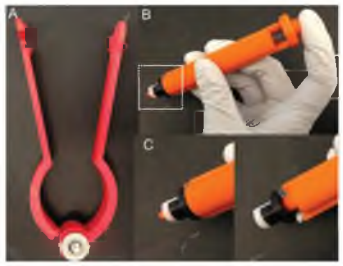

Figure 3 (A) The holder consists of two anchor arms, (B) The anvil tool with engaging ring, (C) A closer look of "Pushing the engaging ring".

Figure 4 (A) Latex tubing was connected with the couplers, (B) ePTFE tubing was connected with the couplers.

The anvil instrument is a pen-shaped rod with an anvil head (Fig. 3(B)). The engaging ring rests on the outside of the anvil rod and can be pushed onto the back ring by sliding the pen cap back and forth. The anvil instrument has two main functions: (i) the outline of the anvil is designed to evert the clipped vessel end (Fig. 2(C)) and (ii) the pen cap pushes the engaging ring onto the back ring such that the clipped vessel end is fixed between the engaging ring and back ring using a friction fit.

C. Mechanical testing

The couplers were tested on both latex tubing and ePTFE tubing with the installation instruments. Latex tubing was selected to simulate the artery due to its relatively similar properties and thick elastic wall. ePTFE was selected to simulate the vein due to its reduced expandability and thin tubing wall. By adjusting the gap between the engaging ring and the back ring, both tubing types were successfully connected with couplers.

A flow test was performed to evaluate the couplers' effects on the flow in the vessel. Two latex tubes were connected with couplers. Another piece of uncut latex tubing with the same length as the coupled one was prepared as a control. Pressurized water was introduced at a rate of 150ml/min- 250 ml/min, which corresponds to a typical range of blood flow rate for arteries with a diameter in the 3-5 mm range, and pushed through both the coupled and control tubes. The pressure before and after the couplers was measured with a pressure gauge.

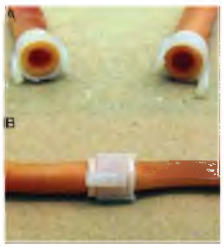

Figure 5 (A) Cross section of human cadaver arterie ends after installation of the engaging ring, (B) Two pieces of human cadaver arteries were connected.

Figure 6 Engaging rings and back rings were manufactured in various sizes for vessels whose outer diameter ranges from 2mm to 6mm.

D. Ex-vivo testing and cadaver animal study

Human cadaver vessels with a 5 mm inner and 6 mm outer diameter were used to test the functionality of the couplers (Fig 5). By adjusting the gap between the engaging ring and the back ring, the couplers are applicable to vessels with different wall thickness.

A qualitative leakage test was performed on two pieces of porcine vessels connected with couplers. One end of the vessel was plugged, and pressurized water was applied from the other end using a syringe. Pressure was increased slowly until the uncoupled portions of the of the vessel expand. Both arteries and veins were tested.

A preliminary study was performed on a cadaver pig using the vascular coupling system and the installation instruments. The aim of the study is to evaluate the functionality of the system in a mock surgery scenario.

III. Results and Discussion

A series of couplers were manufactured and can be used for vessels whose outer diameters are in 2mm-6mm range (Fig 6). Engaging rings were made from both Vero White, a synthetic material used for proof of concept prototyping and PLA with 3D printing techniques. Back rings were made from PMMA with laser cutting.

In testing the functionality of the device, after the engaging ring was installed on the back ring, it was found that the back ring was completely covered with the everted vessel end and was not exposed (Fig 5(A)), the clipped vessel ends were all secured well between the engaging ring and the back ring, leaving a smooth everted vessel intima for the next coupling step.

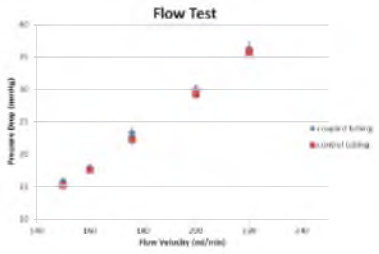

Figure 7 Plot of the flow test data showing the relationship between pressure drop in the tubing versus flow rate across coupled and control tubing.

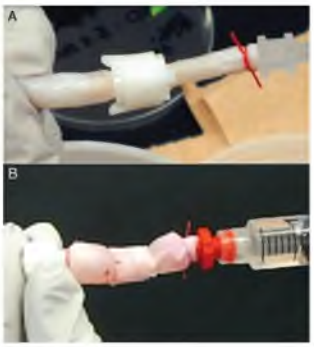

Figure 8 (A) Leakage tests were performed on porcine arteries, (B) Leakage tests were performed on porcine veins.

The coupler flow test results are plotted (Fig. 7) as the pressure difference across the simulated test vessel versus the driving flow rate. The flow test showed that the coupler did not restrict the flow significantly compared to the uncut tubing. These tests were performed multiple times at various flow rates and the differences in pressure drop were minimum, compared with uncut tubing. It can be concluded that the coupler has little effect on the flow.

The coupler leakage test was performed on both porcine arteries and veins. The whole process was recorded and Fig 8 shows the final status of the process. Unbounded portions of the vessel expanded with increasing pressure. There was no leakage found at the coupling point of the vessel during the whole process. A quantitative test is being developed.

A severed renal artery was reconnected in a cadaver pig (Fig 9). The cadaver animal test provided information on the operating abilities of the couplers and the installation instruments in a more realistic environment. The whole anastomosis process was proven to be accomplished in a limited space. In a real surgery, the dimension of the blood vessels will be varying in a certain range. Couplers and instruments that can be used on different sizes of vessels are being developed.

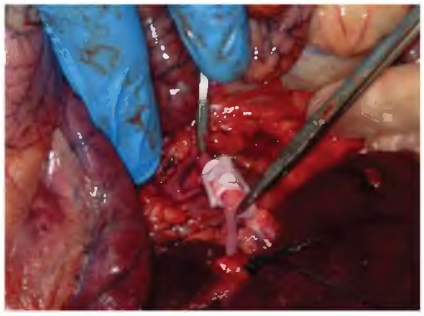

Figure 9 Couplers were installed on the renal arteries in a cadaver pig.

With the new vascular coupling system, the problems of low flexibility and the increased thickness of the arteries are solved and the stress created by everting the end of the artery is relieved by clipping the end of the vessel. Also, by adjusting the gap between the engaging ring and the back ring, the couplers can be used on vessels with the same outer diameter but different wall thickness. The use of couplers without pins reduces the chance of tearing the vessel wall by misplacement of the pins when compared with previous devices that included pins. The proposed device would reduce the time required in the surgery suite and the likelihood of failure of the anastomosis.

IV. Conclusion

A pin-free vascular coupling system and its corresponding instruments were designed, fabricated and tested. The device is easy to use and there is no vessel stretching or damage during the process. The results showed that the new coupler can be used to efficiently perform a vascular anastomosis in cadaver animal models. Future studies will include fabricating the couplers with different biocompatible materials, improving the instruments to adapt to different sizes of vessels and performing *in vivo* tests. The novel vascular coupling system has great potential to be a valuable tool for reconstructive surgery.

Acknowledgment

The authors would like to acknowledge the financial support of Technology Commercialization Project, University of Utah.

References

[1] M. L. Shindo, P. D. Costantino, V. P. Nalbone, D. H. Rice, U. K. Sinha, Use of a Mechanical Microvascular Anastomotic Device in Head and Neck Free Tissue Transfer, Arch Otolaryngol Head Neck Surg, 122, 529-532, 1996

[2] H.E. Kleinert, and M.L. KASDAN, Restoration of blood flow in upper extremity injuries. J Trauma Acute Care Surg. 3, 461-476, 1963.

[3] J. Zdolsek, H. Ledin, D. Lidman, Are mechanical microvascular anastomoses easier to learn than suture anastomoses? Microsurgery. 25, 596-598, 2005.

[4] C.J. Andel, P. V. Pistecky, and C. Borst, Mechanical properties of porcine and human arteries: implications for coronary anastomotic connectors. Ann Thorac Surg. 76, 58-64, 2003.

[5] E. Ferrari, P. Tozzi, and L. K. von Segesser, The Vascular Join: a new sutureless anastomotic device to perform end-to-end anastomosis. Preliminary results in an animal model. Interact Cardiovasc Thorac Surg. 6, 5-8, 2007.

[6] F. Filsoufi, R. S. Farivar, L. Aklog, C.A. Anderson, R.H. Chen, S. Lichtenstein, J. Zhang, and D.H. Adams, Automated distal coronary bypass with a novel magnetic coupler (MVP system). J Thorac Cardiovasc Surg. 127, 185-192, 2004.

[7] J.F. Gummert, U. Opfermann, S. Jacobs, T. Walther, J. Kempfert, F.W. Mohr, and V. Falk, Anastomotic devices for coronary artery bypass grafting: technological options and potential pitfalls. Comput Biol Med. 37, 1384-1393, 2007.

[8] S. Jacobs, F.W. Mohr, and V. Falk, Facilitated endoscopic beating heart coronary bypass grafting using distal anastomotic device. Int. Congr Ser. 1268, 809-812, 2004.

[9] U. Klima, M. Maringka, E. Bagaev, S. Kirschner and A. Haverich, Total magnetic vascular coupling for arterial revascularization. J Thorac Cardiovasc Surg. 127, 602-603, 2004.

[10] C.A. Lally, J. Reid, and P. J. Prendergast, Elastic behavior of porcine coronary artery tissue under uniaxial and equibiaxial tension. Ann Biomed Eng. 32, 1355-1364, 2004.

[11] J.S. Scheltes, C. J. van Andel, P. V. Pistecky, and C. Borst, Coronary anastomotic devices: blood-exposed non-intimal surface and coronary wall stress. J Thorac Cardiovasc Surg. 126, 191-199, 2003.

[12] W.J. Suyker, M.P. Buijsrogge, P.T. Suyker, C.W. Verlaan, C. Borst, and P.F. Grundeman, Stapled coronary anastomosis with minimal intraluminal artifact: The S2 Anastomotic System in the off-pump porcine model. J Thorac Cardiovasc Surg. 127, 498-503, 2004.

[13] K. Ueda, T. Mukai, S. Ichinose, Y. Koyama, and K. Takakuda, Bioabsorbable device for small-caliber vessel anastomosis. Microsurgery. 30, 494-501, 2010.

[14] D.A. Ross, J.Y. Chow, J. Shin, and R. Restifo, Arterial coupling for microvascular free tissue transfer in head and neck reconstruction. Arch Otolaryngol Head Neck Surg. 131, 891-895, 2005.

[15] C. Gehrke, H. Li, H. Sant, B. Gale, and J. Agarwal, Design, fabrication and testing of a novel vascular coupling device. Biomed Microdevices. 16, 173-180, 2014.

Final Design and Development

Reprinted from Journal of Cardiovascular Engineering and Technology, 2015, doi: 10.1007/s13239-015-0220-3 Biomedical Engineering Society

Cardiovascular Engineering and Technology (© 2015)
DOI: 10.1007/s13239-015-0220-3

A Novel Vascular Coupling System for End-to-End Anastomosis

HUIZHONG LI,[1] BRUCE K. GALE,[1] HIMANSHU SANT,[1] JILL SHEA,[2] E. DAVID BELL,[3] and JAY AGARWAL[2]

[1]Department of Mechanical Engineering, University of Utah, 50 S Central Campus Drive Rm 2110, Salt Lake City, UT 84112, USA; [2]Department of Surgery, School of Medicine, University of Utah, 30 N 1900 E, Salt Lake City, UT 84132, USA; and [3]Department of Bioengineering, University of Utah, Salt Lake City, UT 84112, USA

(Received 27 November 2014; accepted 24 February 2015)

Associate Editor Ajit P. Yoganathan oversaw the review of this article.

Abstract—Vascular anastomosis is common during reconstructive surgeries. Traditional hand-suturing techniques are time consuming, subject to human error, and require high technical expertise and complex instruments. Prior attempts to replace hand-suturing technique, including staples, ring-pin devices, cuffing devices, and clips, are either more cumbersome, are unable to maintain a tight seal, or do not work for both arteries and veins. To provide a more efficient and reliable vessel anastomosis, a metal-free vascular coupling system that can be used for both arteries and veins was designed, fabricated and tested. A set of corresponding instruments were developed to facilitate the anastomosis process. Evaluation of the anastomosis by scanning electron microscopy and magnetic resonance imaging, demonstrated that the installation process does not cause damage to the vessel intima and the vascular coupling system is not exposed to the vessel lumen. Mechanical testing results showed that vessels reconnected with the vascular coupling system could withstand 12.7 ± 2.2 N tensile force and have superior leak profiles (0.049 ± 0.015, 0.078 ± 0.016, 0.089 ± 0.008 mL/s at 160, 260, 360 mmHg, respectively) compared to hand sutured vessels (0.310 ± 0.014, 1.123 ± 0.033, 2.092 ± 0.072 mL/s at 160, 260, 360 mmHg, respectively). The anastomotic process was successfully demonstrated on both arteries and veins in cadaver pigs.

Keywords—Microsurgery, Blood vessel, Biocompatible, SEM, MRI.

INTRODUCTION

Vascular anastomosis is common during replantation and free tissue transfer surgeries.[15] The current standard method for microsurgical vascular anastomosis is hand suturing the two cut ends of an artery or vein together using ultrafine techniques with the assistance of an operating microscope.[10] This technique requires specialized training for surgeons, is time consuming with steep learning curves, and is subject to a great degree of human error, like vessel damage or backwall suturing, which might lead to thrombosis and limb or tissue loss, resulting in 2–6% persistent failure rates.[21,22] This could require additional operations and/or amputation, both of which can add to the burden of increasing healthcare costs. Alternative anastomotic devices are highly needed to improve the precision and efficiency of the anastomosis process.

Previous attempts of the anastomotic devices are staples, clips, and cuffing rings,[1,4,5,7,8,11,13,16,19] all of which have fallen short due to the lack of biocompatibility, design flaws and general inefficiency. So far, the most successful approach to simplifying the manual suturing technique exists with ring-pin devices; one of them has been commercialized as the "GEM Microvascular Anastomotic Coupler" (Synovis Micro, Birmingham, AL).[12] This device makes use of two high density polyethylene (HDPE) rings with perpendicularly oriented stainless steel pins which are anchored to the cut ends of two veins. This device is usually used on veins but has a limited role in arterial anastomosis due to increased thickness and higher elasticity of the artery wall. It is very difficult to secure the artery end over the perpendicular pins. Attempts at using this device for arterial anastomosis have only been successful with significant modification of the technique, like using rubber bands to secure the artery end, but this modification undesirably adds time and complexity over traditional manual suturing.[18]

Some of the problems encountered with arterial anastomosis were solved by replacing the rigid ring base with a ring that has rotating wings.[6] While this device works well for arteries, the anastomotic process can still require some manual manipulation of the vessel for consistent pin penetration. Another coupler with both rotating wings and translating pins was designed and largely improved the pin penetration performance.[14] However, it is worth noting that most of

Address correspondence to Huizhong Li, Department of Mechanical Engineering, University of Utah, 50 S Central Campus Drive Rm 2110, Salt Lake City, UT 84112, USA. Electronic mail: lizzylee2526@gmail.com

Published online: 28 February 2015

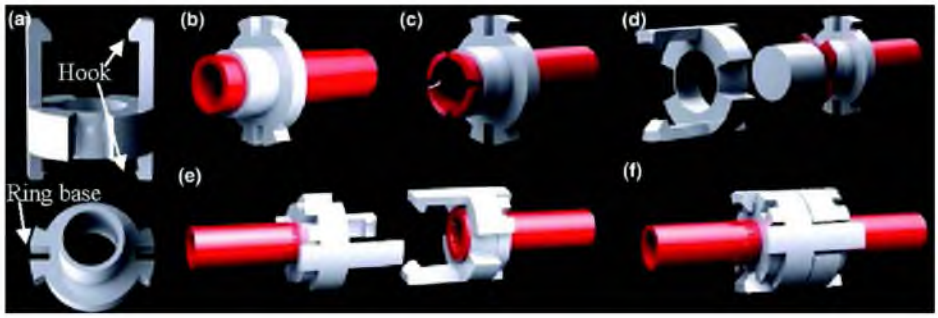

FIGURE 1. Working mechanism of the vascular coupler: (a) The engaging ring and the back ring; (b) The vessel is passed through the back ring; (c) The end of the vessel is clipped 1–2 mm; (d) The vessel end is everted using the temporary placement of an anvil, then the engaging ring slides onto the back ring. This process is performed on both vessel ends; (e) The anvil is removed and two vessel ends with installed engaging rings are ready for connection; (f) Two vessels are connected.

the current anastomotic devices involve the penetration of the vessel wall with metal pins and subsequent eversion of the vessel end. The process of everting the vessel end with attached pins has the potential to stretch the blood vessel wall and cause tearing. Also, the need for metal pins, which are usually made from non-degradable material, makes the potential biodegradability of the devices less feasible. Recently, a hooked device designed for vessels with smaller diameter was introduced. This device was designed without any metal pins and was made from the bioabsorbable material poly(lactide-*co*-glycolide-*co*-caprolactone) (PLGC).[20] However the hooked device design has not progressed as it still requires the inefficient manual eversion of the vessel end and an additional suturing step to secure the vessel onto the device cuff.

Thus, a new vascular coupler that can be used on both arteries and veins while facilitating the manual everting process and avoiding the potential for vessel tearing, will potentially overcome the limitations of previous devices. The vascular coupling system described in this study achieves these design goals and provides an easy and efficient installation process without the use of wall-penetrating pins. A set of installation instruments has been developed to facilitate the anastomosis process. The functionality and feasibility of the vascular coupling system were evaluated through the use of *ex vivo* imaging and mechanical testing. Preliminary studies have been performed on cadaver pigs.

MATERIALS AND METHODS

Vascular Coupler Design and Fabrication

The vascular coupling system, or coupling device, consists of an engaging ring and a back ring for each vessel end, as shown in Figure 1a. The engaging ring has a ring base, on which there are two small cuts and two arms extending longitudinally from the ring base. One long arm extends in the direction of the cut end of the vessel and one short arm extends in the opposite direction. The shorter arm is used to lock the engaging ring to the back ring and the longer arm is used to lock with the mating coupler. There is a hook on the end of each arm for locking purposes, as shown in Figure 1a. The back ring has a ring base and a smooth inner surface to prevent vessel damage, as shown in Figure 1b. The shape of the back ring base is designed to be held with the holder tool. The engaging ring has an inner diameter that is greater than the outer diameter of the back ring, such that the back ring can slide into the inner diameter of the engaging ring.

Coupling device prototypes have been manufactured to establish proof of concept. Engaging rings were built from HDPE using CNC machining. Back rings were built from polymethyl methacrylate (PMMA) using laser cutting.

Application Sequence

To perform a vessel anastomosis: First, one vessel end is passed through the back ring with approximately 2 mm of the vessel extending beyond the edge; Second, the vessel (1–2 mm) end is clipped with four cuts to release the tension around the vessel end in preparation for the everting process; Third, the clipped vessel end is everted with the assistance of an anvil tool and the engaging ring is installed onto the back ring by sliding the back ring into the engaging ring and fitting the back ring base between the short arms on the engaging ring. The same installation steps are performed on the opposite vessel end. When connected, the two

coupling devices are offset by 90° and then locked into each other, wherein the engaging arms of one coupling device extends beyond the back ring of the other coupling device and vice versa, as shown in Figs. 1b–1f. The coupling device is designed to keep the vessel patent at the anastomosis, while preventing any device parts from coming in contact with blood flowing through the vessel, which not only reduces the chance of blockage or collapse at the point of coupling, but reduces the risk of thrombosis.[3]

Installation Tools

While it is possible to use standard surgical instruments to accomplish the steps necessary for anastomosis, a set of instruments aimed at facilitating the anastomosis process using the coupling devices have been developed. The instrument set includes a holder tool and an anvil tool, as shown in Figure 2.

Holder Tool

The function of the holder tool is to hold the back ring. In the holder tool, the two anchor arms are connected using the pinned hinge at the end (Figure 2b). On each anchor arm, there is a clip installed at the head of the anchor to hold and release the back ring by a spring (Figure 2a). The clip is exchangeable for different sizes. The difference between the two anchors is that the heads are offset from each other by 90° to allow the two couplers held by the instruments to be locked with each other at the completion of the anastomosis process.

Anvil Tool

There are two functions of the anvil tool: everting the clipped vessel end and installing the engaging ring onto the back ring. The anvil tool is a retrofitted syringe with an anvil head, as shown in Figure 2c. The engaging coupler rests on the outside of the anvil rod and can be pushed by sliding the syringe plunger (Figure 2e). The contour of the anvil head is designed to evert the clipped vessel end when inserted into the vessel lumen and the syringe plunger pushes the engaging coupler onto the back ring such that the clipped vessel end is fixed between the engaging coupler and back ring by friction.

Ex vivo Testing

A series of tests were performed *ex vivo* on porcine vessels to evaluate the operating abilities of the vascular coupling systems. SEM and MRI imaging were utilized to determine if there was intimal damage during the installation process, if the back ring could be fully covered by the everted vessel end and if any foreign device material was in the lumen of the vessel after coupling. The mechanical tests included a tensile test to determine the strength of the interface between the two coupled vessels and a leakage test to measure leaks associated with the coupling devices.

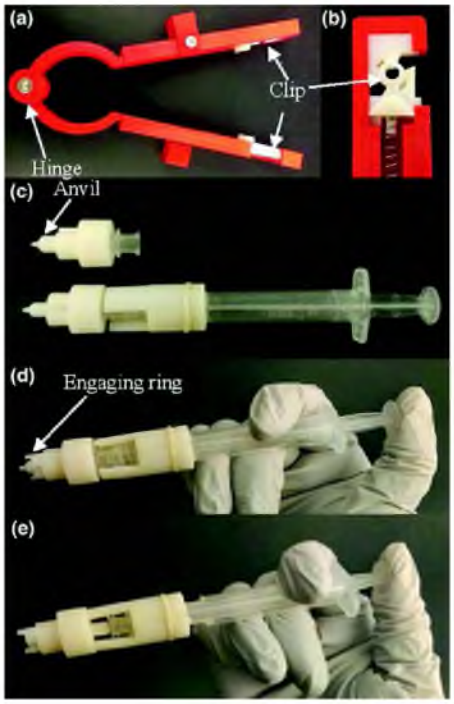

FIGURE 2. Installation tools: (a) The holder tool; (b) The head of the holder tool, the back ring is secured with clip; (c) The anvil tool with different sizes of anvils; (d) The engaging ring rests on the anvil (before pushing); (e) The engaging ring slides along the anvil (after pushing).

SEM Imaging

After the engaging ring is installed on the back ring, the clipped vessel end is everted and fit into the gap between the two rings. During the installation process, the everted vessel end should completely cover the back ring to prevent foreign material from being exposed to the vessel lumen and the process should not cause any damage to the vessel intima. SEM was used to evaluate the everted vessel intima after connecting the engaging ring onto the back ring. In the test, a segment of carotid artery (5 mm OD and 4 mm ID) harvested from a Yorkshire swine (Female,

11–12 weeks old, 40–45 kg) was passed through the back ring, then the vessel end was clipped and everted by installing the engaging ring (Images are shown in Figure 4). The prepared vessel sample was stabilized on a holder and the cross section imaged with SEM (FEI Quanta 600 FEG, SEM) to detect if there was vessel damage and if the back ring was fully covered. The designated acceleration voltage was 15.00 kV and the working distance was 36.2 mm. Both secondary electron and backscattered electron images were taken during the scanning.

MRI Imaging

MRI was used to evaluate the connected vessel lumen and the status of the everted vessel ends. The everted vessel end should be secured between the engaging ring and the back ring, and the device should not be exposed in the vessel lumen. In this test, two segments of porcine carotid arteries (5 mm OD and 4 mm ID) were reconnected with the vascular coupling systems. Then the two free ends of the coupled arteries were sutured on Luer connectors and placed in a larger tube to protect against leakage during MRI imaging. Imaging experiments were conducted on a 7-Tesla Bruker Biospec MRI scanner (Bruker Biospin Inc., Ettlingen, Germany), interfaced with 12-cm actively shielded gradient insert capable of producing a magnetic field gradient of 600 mT/m. A 50 mm inner diameter quadrature volume RF coil (Rapid MRI inc) was used for MR signal transmission and reception. A multi slice fast spin echo pulse sequence was used to obtain complete coverage of the coupling system with the following parameters: 2000 ms repetition time, 35 ms echo time, 4 lines per excitation, 4 averages, 10 slices 30 mm × 30 mm field-of-view, 128 × 96 matrix, yielding in-plane resolution of 234 μm × 312 μm, scan time of 3 min.

Tensile Test

Blood vessels in the human body are subject to a degree of tension and stretching due to daily movement. The purpose of the tensile test was to evaluate the highest force a coupled blood vessel could withstand. Harvested carotid arteries (sheep; $n = 6$) were cut in half and then reconnected with the coupling devices. The coupled artery was then mounted to an arterial tensile testing machine, similar to a previously described system.[2] Briefly, both ends of the coupled carotid arteries were cannulated with 1/16 inch hose barbs, and secured with size 2 silk suture and cyanoacrylate glue. The hose barbs, and the associated fixtures, were attached to a custom vertical linear stage (Parker Automation, Cleveland, OH). The upper fixture is suspended from a 10 lbs capacity load cell (Model MDB-10, Transducer Techniques, Temecula, CA) through an X–Y stage (MS-125-XY, Newport, Irvine, CA) that allows for correction of any barb misalignment. The lower fixture was mounted rigidly to the stage. Displacement of the stage translated both fixtures equally in opposite directions, ensuring the coupler remained stationary in space. Specimens were viewed *via* a digital video camera (PL-A641, Pixelink, Ottawa, Canada) equipped with a zoom lens (VZM450i, Edmund Optics, Barrington, NJ). Test control, as well as data and video acquisition, were accomplished using a custom LabVIEW program (National Instruments, Austin, TX). Linear stage positions were given by digital encoders (resolution 1.0 μm). Vessels were kept hydrated with Hanks Buffered Saline Solution (HBSS; KCl 5.37, KH_2PO_4 0.44, NaCl 136.9, Na_2HPO_4 0.34, D-glucose 5.55, $NaHCO_3$ 4.17; concentrations in mM) until mounting to the test device and were then immediately pulled axially, quasi-statically, from a buckled configuration to failure.

Leak Test

The vascular coupling system should keep the anastomosis sealed under normal physiologic blood pressure range. In this test, two experiments (open end and sealed end) were set up to compare the anastomosis seal of both coupled and hand-sutured vessels. The structural integrity of the coupled and hand anastomoses were compared using *ex vivo* carotid arteries harvested from Yorkshire swine (Female, 11–12 weeks old, 40–45 kg). One carotid artery was reconnected with the coupling device and the other was hand sutured by a skilled microsurgeon (co-author; JA). In the open end experiment, one artery end was connected to a reservoir filled with water and the other end was connected to a beaker. The water in the reservoir was pressurized to three different levels corresponding to an extended range of acceptable blood pressures (160, 260, 360 mmHg), and the pressurized water flowed through the coupled/sutured artery to a beaker. Afterwards, air with corresponding pressures (160, 260, 360 mmHg) was sent through the coupled/sutured artery to make sure there is no residual water left in the testing arteries. The driving pressure was measured with a pressure gage (WIKA Instruments, Model 111.25 CT, GA). The initial amount of water in the reservoir and the final amount of water in the beaker were compared and recorded to determine how much water was lost in the flowing process. In the sealed end experiment, one end of the artery was connected to a reservoir filled with water and the other end was plugged. Pressurized water (160, 260, 360 mmHg) was pushed into the coupled/sutured arteries for the same amount of time. The amount of water that leaked from the arteries was recorded and

the leak rates were calculated and compared. Additionally, to check where the leaks were, the coupled/sutured arteries were placed under water and air was sent through the vessel. Leak locations were indicated by escaping bubbles. The open end and sealed end tests were both performed three times for each artery at each pressure.

Cadaver Animal Testing

To evaluate the functionality of the vascular coupling system in a mock surgery scenario, preliminary anastomosis surgeries were performed on cadaver pigs (3 month old Yorkshire cross-domestic swine; ~30 kg; $n = 2$) using the coupling devices and accompanying installation instruments. All animal work was performed using protocols approved by the Institutional Animal Care and Use Committee at the University of Utah. The carotid arteries and jugular veins were clamped by vessel clamps at each end and then cut in half. The vessel anastomoses are performed by a microsurgeon (co-author, JA) with the vascular coupling system following the user-instructions. Once the blood vessels were reconnected, the clamps were removed.

RESULTS

Fabrication Results

Figure 3 shows the HDPE engaging rings fabricated using CNC machining and the PMMA back rings fabricated using laser cutting. Both engaging rings and back rings have been made for blood vessels with 3, 4, and 5 mm outer diameters.

Ex vivo Testing Results

SEM Imaging

As can be seen in the cross sectional images of two vessel ends with an installed back ring and an engaging ring (Figure 4a), the clipped vessel end has been fully everted and secured between the engaging ring and the back ring. Figures 4c and 4d shows the SEM images of porcine arteries after the engaging rings were installed on the back rings. No damage is seen on the vessel intima after the everting process. Further, the back ring is fully covered by the smooth and consistent vessel intima (Figure 4c), in preparation for the next intima-to-intima coupling step (Figure 4b).

FIGURE 3. HDPE engaging rings and PMMA back rings.

MRI Imaging

Figure 5 shows the coupled porcine arteries and the corresponding axial MRI image of the coupled arteries. The MRI images show the everted vessel ends compressed between the engaging ring and the back ring. The two vessel ends are pressed against each other and there is no foreign body exposed in the vessel lumen.

Tensile Test

Figure 6 shows the stretching process of sheep arteries ($n = 6$). At the beginning, the artery was slack and there was no tensile force applied to it. At the end, the artery was pulled to failure. There were three main failure modes in these tensile tests: (1) the artery end slipped off the Luer connector, (2) the back ring slipped off the corresponding engaging ring and (3) the artery end tore off the back ring.

The results showed that the force the six coupled arteries could withstand was 12.7 ± 2.2 N. Under normal physiological load (13.3 kPa), the axial stress on blood vessel walls is around 13 kPa and 50 kPa at 0 and 20% elongation, respectively,[9,17] which corresponds to 0.17 and 0.64 N for a 5 mm outer and 3 mm inner diameter blood vessel. Under extreme physiological conditions with a 30 kPa blood pressure and 20% axial stretch,[17] the axial stress is around 112 kPa and the corresponding axial force is 1.4 N. In both scenarios, the maximum force the coupled arteries can withstand is much higher than the possible physiological load in the human body.

Leak Test

For the open end experiment, there were no noticeable leaks found for both hand sutured and coupled vessels under three pressures (160, 260, 360 mmHg). For the sealed end experiment, leaks were found on both hand sutured and coupled vessels. The leak rates for both vessels under the three pressures are plotted in Figure 7. The leak rates of hand sutured vessels (0.310 ± 0.014 mL/s at 160 mmHg, 1.123 ± 0.033 mL/s at 260 mmHg, 2.092 ± 0.072 mL/s at 360 mmHg) increase with pressure and are larger

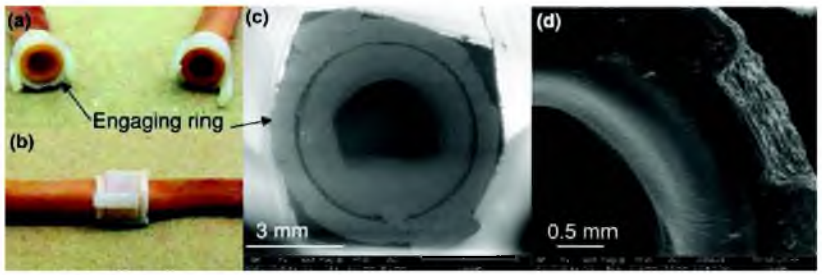

FIGURE 4. (a) Two human cadaver artery ends with installed back rings and engaging rings ready for reconnection; (b) Reconnected arteries; (c) SEM image of the vessel end cross section; (d) Zoomed in view of the vessel in image (c).

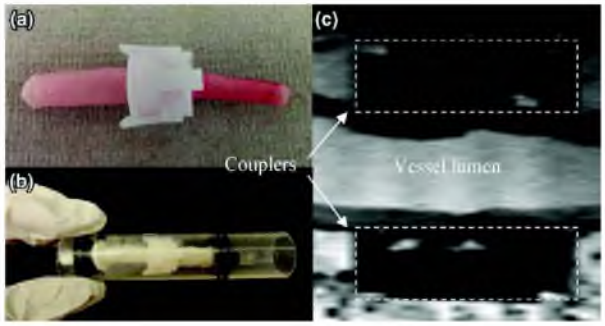

FIGURE 5. (a) Coupled porcine arteries; (b) Coupled porcine arteries stabilized inside a protective tube; (c) MRI image along the flow-axis of the coupled porcine arteries.

than in the coupled vessels (0.049 ± 0.015 mL/s at 160 mmHg, 0.078 ± 0.016 mL/s at 260 mmHg, 0.089 ± 0.008 mL/s at 360 mmHg). The difference of leak rates between coupled and sutured vessels are significant ($p = 0.003$, 0.001, 0.0006 at 160, 260, 360 mmHg, respectively). No swelling of arteries was found for both open end and sealed end tests.

Cadaver Animal Testing Results

Both jugular veins (Figure 8a) and carotid arteries (Figure 8b) were successfully reconnected with the vascular coupling system and its corresponding tools. For the carotid artery anastomoses, the contralateral carotid artery included a graft to mimic the scenario where a graft is needed. Once trained on how to operate the vascular coupling device, it was possible for a researcher to successfully connect the artery and vein using the device. The entire process for each anastomosis took less than three minutes, which is much shorter than hand suturing (20–40 min) using interrupted techniques.

DISCUSSION

The vascular coupling system in this study has been successfully demonstrated to be a potential approach for end-to-end anastomosis. It not only meets the necessary requirements to withstand corresponding physiological conditions, but also has several advantages enabling it to produce a faster and more efficient anastomosis compared to hand suturing and other existing methods. For example, the new design in this study simplifies the manual eversion process and can release tension in the vessel wall by clipping the vessel end, thus reducing the potential for vessel-end tearing. The gap between the back ring and the engaging ring can be adjusted for vessels with various wall thicknesses, which makes the reconnection of two vessels

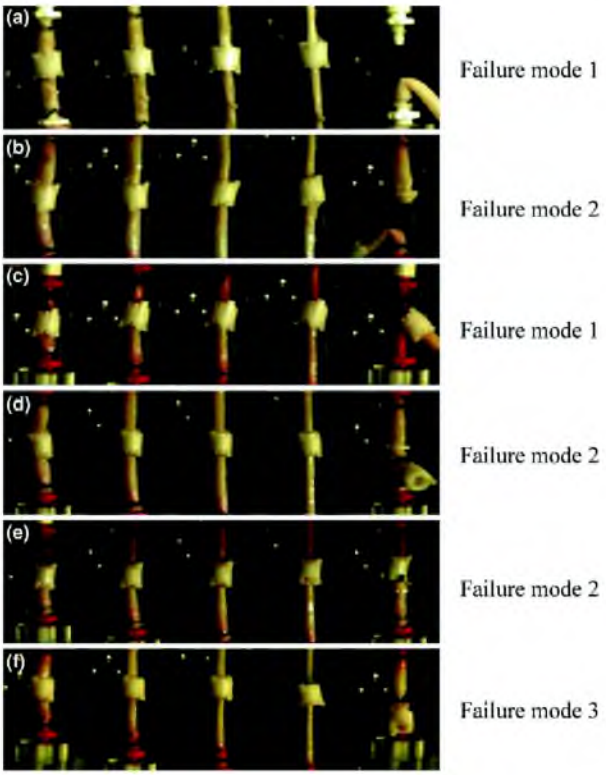

FIGURE 6. Images of the tensile testing of the six sheep arteries from the start to failure. Failure mode 1: artery end slipped off the Luer connector; Failure mode 2: the back ring slipped off the corresponding engaging ring; Failure mode 3: the artery end tore off the back ring.

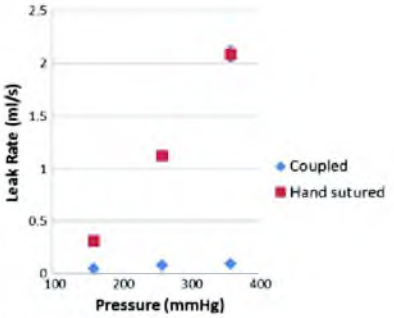

FIGURE 7. Leak rates of coupled and hand sutured vessels under three pressures for sealed end vessels.

with the same outer diameter, but different wall thickness easy and possible. The development of corresponding tools for use with the coupler has also been important to the anastomosis efficiency of the vascular coupling system. The holder tool can hold the back ring tightly and the clip-spring mechanism makes it easy to exchange back rings of different size, allowing for adjustment of the device for different vessel wall thickness. The shape of the anvil head is specifically designed so that the vessel end can automatically be opened and everted once the anvil tool is inserted into the vessel lumen. Using the developed tools, a surgeon can perform the anastomosis in a series of simple steps.

The couplers have been manufactured in various sizes to accommodate vessels with a range of dimensions. HDPE was selected to build the engaging rings as it not

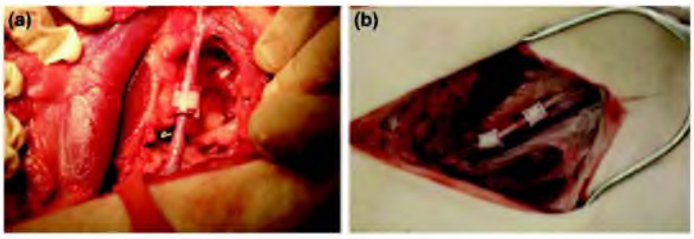

FIGURE 8. (a) Reconnected jugular veins; (b) Reconnected carotid arteries.

only provides the flexibility needed in the bending arms during the locking process, but also has the strength to ensure a tight lock. PMMA was selected to build the back rings because of its compatibility with laser machining, which makes the prototyping process quick and easy. In the future, these components could be made of biodegradable materials to allow elimination of the coupler once the vessel is strong enough. A polylactic acid (PLA) coupling prototype using a 3D printing technique has been manufactured as proof of principle and will be tested in the future.

The *ex vivo* testing and cadaver animal studies were designed to predict and verify the performance and properties of the vascular coupling system in preparation for live animal studies. The vascular coupling systems were found to provide a quick end-to-end anastomosis in a mock surgery scenario in a convenient and reliable way. Analysis of the coupled vessels using SEM and MRI images showed that there was no damage to the vessel intima during the installation process and no foreign body was in the vessel lumen. The tensile test results demonstrated that the coupled vessels can withstand much higher forces than the normal physiologic load on blood vessels in the human body. The leak test compared the leak rate of coupled vessel and hand-sutured vessel and showed that though both hand sutured and coupled vessels leaked during the mechanical test, the leak rate with the coupler was lower. It is known that in real physiologic scenarios, platelets in the blood will help to seal any small leaks, as is seen with the small holes produced when suturing blood vessels. Thus, the leaks associated with the coupled vessels should not be a problem *in vivo*. Torque may be applied to arteries during movements; for example, the carotid artery experiences torsion during head movements. The torque is expected to be relatively low and the vessels are likely to experience most of the torsion rather than the couplers, as the stiffness of the materials is significantly different. The effects of torsion on the commercial Synovis coupler have not been reported to our best of knowledge, nor have they been shown to be a concern.

CONCLUSION

In conclusion, a novel vascular coupling system for both arteries and veins along with a set of installation tools specifically designed for end-to-end anastomosis have been successfully developed, fabricated and tested. The vascular coupling system is easy to use and demonstrates no intimal damage and an absence of foreign material in the vessel lumen as seen with SEM and MRI imaging. The mechanical testing proves that the coupling system not only has the ability to withstand 12.7 ± 2.2 N tensile force, which is much higher than normal loads on blood vessels in the body, but also has superior leak profiles compared to hand suturing under an extended range of normal blood pressures. The vascular coupling system has been successfully demonstrated in cadaver animals. The implementation of the current coupling system requires less than three minutes to complete an anastomosis in a mock surgery scenario with minimal training. With minor improvements, the vascular coupling system has great potential as an implantable anastomotic device to be used in future reconstructive surgeries.

ACKNOWLEDGMENTS

The authors would like to acknowledge Patti Larrabee and Hannah Beal for their help in harvesting blood vessels used in the cadaver animal study. The authors also would like to acknowledge the use of the College of Engineering Nanofabrication Lab and the Small Animal Imaging Facility at the University of Utah, and the financial support from the Technology and Venture Commercialization Office at the University of Utah, and the State of Utah Governor's Office for Economic Development.

CONFLICT OF INTEREST

Huizhong Li, Bruce K. Gale, Himanshu Sant, Jill Shea, E. David Bell and Jay Agarwal declare that they have no conflict of interest.

STATEMENT OF HUMAN STUDIES

No human studies were carried out by the authors for this article.

STATEMENT OF ANIMAL STUDIES

No animal studies were carried out by the authors for this article.

REFERENCES

[1]Andel, C. J., P. V. Pistecky, and C. Borst. Mechanical properties of porcine and human arteries: implications for coronary anastomotic connectors. *Ann. Thorac. Surg.* 76:58–64, 2003.

[2]Bell, E. D., R. S. Kunjir, and K. L. Monson. Biaxial and failure properties of passive rat middle cerebral arteries. *J. Biomech.* 46:91–96, 2013.

[3]Chernichenko, N., D. A. Ross, J. Shin, J. Y. Chow, C. T. Sasaki, and S. Ariyan. Arterial coupling for microvascular free tissue transfer. *Otolaryngol. Head Neck Surg.* 138:614–618, 2008.

[4]Ferrari, E., P. Tozzi, and L. K. von Segesser. The vascular join: a new sutureless anastomotic device to perform end-to-end anastomosis. Preliminary results in an animal model. *Interact. Cardiovasc. Thorac. Surg.* 6:5–8, 2007.

[5]Filsoufi, F., R. S. Farivar, L. Aklog, C. A. Anderson, R. H. Chen, S. Lichtenstein, J. Zhang, and D. H. Adams. Automated distal coronary bypass with a novel magnetic coupler (MVP system). *J. Thorac. Cardiovasc. Surg.* 127:185–192, 2004.

[6]Gebrke, C., H. Li, H. Sant, B. Gale, and J. Agarwal. Design, fabrication and testing of a novel vascular coupling device. *Biomed. Microdevices.* 16:173–180, 2014.

[7]Gummert, J. F., U. Opfermann, S. Jacobs, T. Walther, J. Kempfert, F. W. Mohr, and V. Falk. Anastomotic devices for coronary artery bypass grafting: technological options and potential pitfalls. *Comput. Biol. Med.* 37:1384–1393, 2007.

[8]Jacobs, S., F. W. Mohr, and V. Falk. Facilitated endoscopic beating heart coronary bypass grafting using distal anastomotic device. *Int. Congr. Ser.* 1268:809–812, 2004.

[9]Khamdaeng, T., J. Luo, J. Vappo, P. Terdtoon, and E. E. Konofagou. Arterial stiffness identification of the human carotid artery using the stress–strain relationship in vivo. *Ultrasonics.* 52:402–411, 2012.

[10]Kleinert, H. E., and M. L. Kasdan. Restoration of blood flow in upper extremity injuries. *J. Trauma Acute Care Surg.* 3:461–476, 1963.

[11]Klima, U., M. Maringka, E. Bagaev, S. Kirschner, and A. Haverich. Total magnetic vascular coupling for arterial revascularization. *J. Thorac. Cardiovasc. Surg.* 127:602–603, 2004.

[12]Lally, C., F. Dolan, and P. J. Prendergast. Cardiovascular stent design and vessel stresses: a finite element analysis. *J. Biomech.* 38:1574–1581, 2005.

[13]Lally, C., A. J. Reid, and P. J. Prendergast. Elastic behavior of porcine coronary artery tissue under uniaxial and equibiaxial tension. *Ann. Biomed. Eng.* 32:1355–1364, 2004.

[14]Li, H., C. Gehrke, H. Sant, B. K. Gale., and J. Agarwal. A new vascular coupler design for end-to-end anastomosis: fabrication and proof-of-concept evaluation, 2014 (accepted).

[15]Ross, D. A., J. Y. Chow, J. Shin, and R. Restifo. Arterial coupling for microvascular free tissue transfer in head and neck reconstruction. *Arch. Otolaryngol. Head Neck Surg.* 131:891–895, 2005.

[16]Scheltes, J. S., C. J. van Andel, P. V. Pistecky, and C. Borst. Coronary anastomotic devices: blood-exposed non-intimal surface and coronary wall stress. *J. Thorac. Cardiovasc. Surg.* 126:191–199, 2003.

[17]Sommer, G., P. Regitnig, L. Költringer, and G. A. Holzapfel. Biaxial mechanical properties of intact and layer-dissected human carotid arteries at physical and supraphysical loadings. *Am. J. Physiol. Heart Circ. Physiol.* 298:898–912, 2010.

[18]Spector, J. A., L. B. Draper, J. P. Levine, and C. Y. Ahn. Routine use of microvascular coupling device for arterial anastomosis in breast reconstruction. *Ann. Plast. Surg.* 56:365–368, 2006.

[19]Suyker, W. J., M. P. Buijsrogge, P. T. Suyker, C. W. Verlaan, C. Borst, and P. F. Grundeman. Stapled coronary anastomosis with minimal intraluminal artifact: The S2 Anastomotic System in the off-pump porcine model. *J. Thorac. Cardiovasc. Surg.* 127:498–503, 2004.

[20]Ueda, K., T. Mukai, S. Ichinose, Y. Koyama, and K. Takakuda. Bioabsorbable device for small-caliber vessel anastomosis. *Microsurgery.* 30:494–501, 2010.

[21]Yajima, K., Y. Yamamoto, K. Nohira, Y. Shintomi, P. N. Blondeel, M. Sekido, W. Mol, M. Ueda, and T. Sugihara. A new technique of microvascular suturing: the chopstick rest technique. *Br. J. Plast. Surg.* 57:567–571, 2004.

[22]Zdolsek, J., H. Ledin, and D. Lidman. Are mechanical microvascular anastomoses easier to learn than suture anastomoses? *Microsurgery.* 25:596–598, 2005.

CHAPTER 5

INITIAL LIVE ANIMAL STUDY

Abstract

A clinical animal study was performed to evaluate the abilities of the vascular coupling device and its corresponding tools developed in Chapter 4. A segment of ePTFE tubing was placed using two couplers as a graft to reconnect the carotid arteries of a pig. Two end-to-end anastomoses were accomplished. Ultrasound images were taken to evaluate the blood flow at the anastomotic site right after the surgery, one week and two weeks after the surgery. MRI images were also taken after two weeks of the surgery to demonstrate there is no foreign body in the vessel lumen.

Materials and Methods

For an animal to be used as a model for the vascular coupling device, its blood vessels must be large enough for the creation of anastomoses of the arterial and venous vessels. As the size of the blood vessels of rabbits, rats, or mice are too small, these animal models were not used. Pigs have been used in cardiovascular research for decades and are considered an excellent large animal model in this domain. Many

biological reagents are readily available for pig. The live animal study uses pigs of Yorkshire cross domestic strain.

A 3-month swine (Yorkshine, 25-30 kg) received general anesthesia and sterile conditions. The carotid artery was exposed through incisions on one side of the neck. The carotid artery was clamped using microvessel clamps at the proximal and distal end. A cut was made around the middle point of the artery. One end of an expanded polytetrafluoroethylene (PTFE) graft (3.5-mm internal diameter, 4-cm length) (Zeus, Inc) was connected to the proximal end of the artery and the other end of the graft was connected to the distal end of the artery using the vascular coupling devices. Once both anastomoses were completed, microclamps were released at the same time to allow blood flowing through. After graft patency and hemostasis was assured, the surgical wounds was sutured closed and the wound will be wiped with povidone-iodine. The following medications were administered to assist in postoperative pain control: Buprenorphine (0.05-0.1 mg/kg) IM, once before surgery (duration 10-12 h); Fentanyl patch (50 ug/pig) transdermal, continuous delivery for 72 hours. The antibiotic Baytril (enrofloxacin, 5 mg/kg) were administered IM one time a day for three days starting preoperatively to prevent infections. Carprofin (2-4.4 mg/kg, IM) may also be delivered if needed for swelling at the incision site. The swine received observation twice a day for first 72 hours post-surgery and once a day after that time frame.

A portable duplex ultra sound machine was used postoperatively to monitor blood flow across the anastomoses. The scanning was performed on post-op day 0, day 7, day 14 prior to device explant. The data from the ultrasound were used to determine patency

of the vessels at each time point. MRI was also used to evaluate the vessel lumen after surgery.

Results

In the animal model, the carotid artery was successfully reconnected by a segment of ePTFE graft with the vascular coupling devices and their corresponding tools. No active bleeding was observed after the anastomoses were completed. The surgery process is shown in Figure 5.1. The ultrasound images and MRI images confirmed good anastomotic results. The anastomoses obtained good patency and no adverse foreign body response or failures in the vessel were detected right after the surgery. Ultrasound images were also obtained at one week and two weeks after the surgery. The results showed that the patency is still acceptable one week after the surgery. Two weeks after surgery, however, the blood flow information is not very clear from the ultrasound image, suggesting there might be a clot in the vessel lumen. The ultrasound images are shown in Figure 5.2 and the MRI images is shown in Figure 5.3.

Discussion and Conclusion

The vascular coupling device and its corresponding tools have proved to be an efficient method to perform end-to-end anastomosis in live animal model. The set of vascular coupling system simplifies and standardizes the vascular anastomosis process. The anastomoses on the carotid arteries are successful and the pig has survived for a month after the surgery prior being sacrificed. The anastomoses have achieved good patency in the first week. The insufficient blood flow information during the second

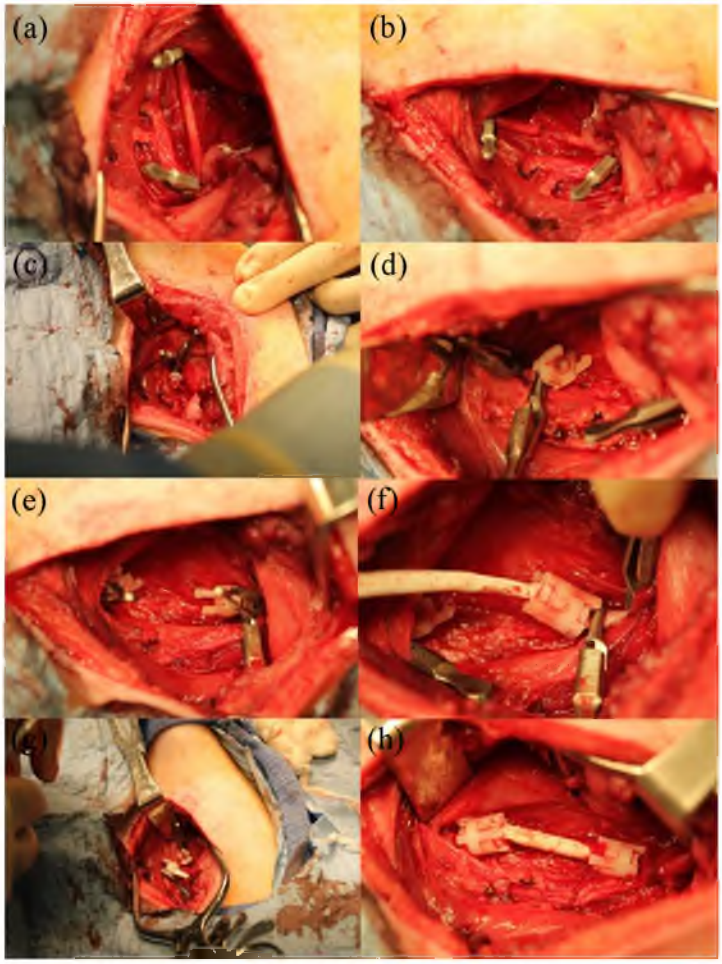

Figure 5.1. The anastomosis process on the carotid artery: (a) A carotid artery; (b) A cut made on the carotid artery; (c) One end of the carotid artery sent through the inner ring; (d) The engaging ring installed on the inner ring; (e) Vascular coupling devices installed at both ends of the carotid arteries; (f) One end of the PTFE graft connected with one end of the artery; (g) The other end of the PTFE graft ready for connection; (h) Two anastomoses completed with the PTFE graft.

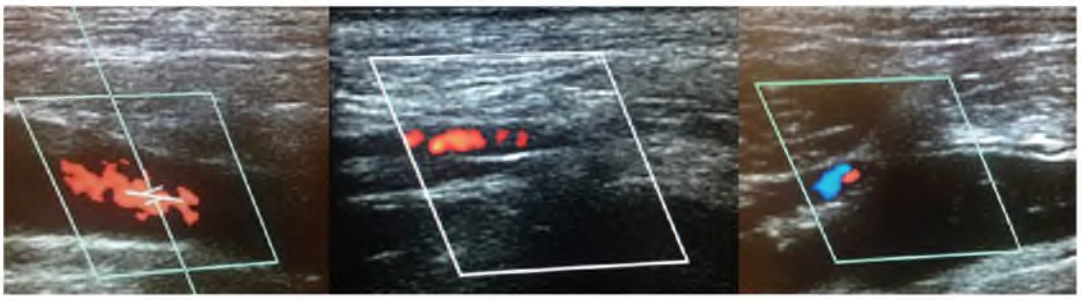

Figure 5.2. The color-Doppler shows pulsatile flow in the vessel (from left to right): Day 0, Day 7, and Day 14 after the surgery.

Figure 5.3. MRI image at approximately three weeks after surgery shows a uniform tissue in the vessel and the couplers are still present.

week suggests there might be clotting in the vessel lumen. The reason for the clotting might be the mismatched size and wrinkled PTFE tubing. However, as the initial animal study, the vascular coupling system has demonstrated its high efficacy and easy-to-use ability, which will be helpful to the following experimental clinical studies.

CHAPTER 6

CONCLUSIONS, CONTRIBUTIONS, AND FUTURE WORK

The dissertation reports on the design, fabrication, modeling, and testing of two vascular coupling devices. This chapter lists the conclusions, contributions, and opportunities for further work related to these devices.

Conclusions

Vascular Coupling Device with Pins

- A ring-pin coupler with four rotatable wings and four translatable pins was selected as the optimal design due to the lower strain of the vessel wall during the stretching process, the convenience of installation and alignment, and the ability to provide an intima-to-intima anastomosis.
- The geometric features of the coupler, such as the wing pivot point and pin offset, significantly increased the vessel strain and/or vessel slipping during the installation process and should be minimized as much as possible.
- The scaled coupler designs for blood vessels with different geometries clearly illustrated that merely scaling down the device will not be sufficient. Additional

force, tools, or friction between the pin and the vessel wall will be required for successful intima-to-intima anastomosis.

- The vascular coupler with rotatable wings and translatable pins and a set of installation tools specifically for end-to-end anastomosis have been successfully designed, fabricated, and tested to show proof-of-concept of the design.
- The vascular coupler is easy to use and demonstrates zero leakage under physiological conditions, minimal to no effect of flow, and the ability to withstand high separation force.
- Both the modeling and the *ex vivo* testing results show that the vascular coupler could open the vessel end without damaging it. Modeling results and *ex vivo* tests suggest that the vessels should withstand the forces applied by the coupler and that might be found in the body.
- With minimum training, the implementation of the current device requires less than three minutes to complete an end-to-end anastomosis.

Vascular Coupling Device without Pins

- A vascular coupling system for both arteries and veins along with a set of installation tools specifically designed for end-to-end anastomosis have been successfully developed, fabricated, and tested.
- The vascular coupling system is easy to use and demonstrates no intimal damage and an absence of foreign material in the vessel lumen as seen with SEM and MRI imaging.
- The mechanical testing proves that the coupling system not only has the ability to

withstand 12.7 ± 2.2 N tensile force, which is much higher than normal loads on blood vessels in the body, but also has superior leak profiles compared to hand suturing under an extended range of normal blood pressures.

- The vascular coupling system has been successfully demonstrated in cadaver animals. The implementation of the current coupling system requires less than three minutes completing an anastomosis in a mock surgery scenario with minimal training.

Contributions

- Two solid designs of vascular coupling devices for end-to-end anastomosis have been achieved. Both designs have all of the necessary functional components to not only provide a safe and effective vascular anastomosis compared to previous methods, but provide strong fundamentals for future application. With further manufacturing development to allow mass production and meet appropriate regulatory guidelines, the vascular coupler will achieve its potential as an implantable end-to-end anastomosis device and make a valuable tool for the medical community.
- A finite element model was built to simulate the vessel-device interaction. The optimization process of the vascular coupling device using FEM, which includes model building, meshing, material selecting, and boundary conditions applying, can be extended to other devices involving vessel-device interaction.
- A variety of rapid prototyping techniques have been developed during this dissertation. These techniques can be applied on the prototyping process of many

different devices. Laser cutting was used to fabricate complex 3D features and other mechanical structures like plastic hinges. The compatibility of different material with laser cutting will be useful for future application. A manual tool set to build prototypes from soft materials (HDPE) has been created to perform quick and easy prototyping.

- A series of mechanical testing to evaluate the vascular anastomosis performance has been designed. These bench testing methods are essential to determine the quality of anastomotic devices and can be set as standard criteria to evaluate if the anastomotic device is ready for further animal studies.

Future Work

There are six directions for the further studies about the vascular coupling device: animal study, biodegradable devices, and end-to-side application. Each of this direction is based on the findings from the current study.

The first direction is animal study using the vascular coupling device in Chapter 4. The installation tools that have developed need further simplification to be more user-friendly and less cumbersome. In addition, metal tools are preferred in the long-term animal study for strength and easy cleaning. These considerations are crucial for the future success of this device.

The second direction is biodegradability of the device. The vascular coupling device developed in Chapter 4 has the potential to be developed as biodegradable device since there is no metal or pins involved. Material like Polylactic acid (PLA), Poly(Lactide-co-Glycolide) (PLGA), and other bioabsorbable polymer could be used to build the

prototypes by 3D printing, injection molding, or other manufacturing methods. *Ex vivo* biodegradation testing of the device and the joint strength changing with material degrading are also worth evaluating.

The third direction is end-to-side application. It would be a great benefit for the medical community if the same devices or similar devices can be applied in the end-to-side scenarios as well. The same design requirements and principles used in developing the current end-to-end vascular coupling devices will be helpful for the end-to-side or even side-to-side application.

The fourth direction is blood flow modeling with the vascular coupling device. The effects of the vascular coupling device on blood flow in artery would be an interesting topic to explore. First, as the compliance of the artery is reduced at the anastomotic site because of the rigid coupling device, the effects of the less-compliant vessel wall on blood flow might cause higher shear stress. Second, as the coupler size is discrete, the mismatch between the coupler and the blood vessel is also worth exploring.

The fifth direction is a compliant vascular coupling device. A compliant vascular coupling device will not limit the elasticity of the vessel wall at the anastomotic site and will have fewer effects on blood flow.

The sixth direction is adding drug delivery functionality into the vascular coupling device. Eluting drug can aid blood vessel regrowth and prevent infection at the anastomotic site.